ELSEVIER

Catalysis Today 51 (1999) 3–23

CATALYSIS TODAY

Forty years of applied catalysis research at Xiamen University and its interaction with fundamental catalysis research

K.R. Tsai*, D.A. Chen, H.L. Wan, H.B. Zhang, G.D. Lin, P.X. Zhang

Department of Chemistry and Institute of Physical Chemistry, State Key Laboratory for Physical Chemistry of Solid Surfaces, Xiamen University, Xiamen 361005, China

Abstract

This paper gives a concise, chronological review of 40 years of applied catalysis research done at Xiamen University, in acetylene and olefin conversion, nitrogen fixation, and in more detail CO hydrogenation to methanol and ethanol, oxidative coupling of methane, and oxidative dehydrogenation of light alkanes; some references of more recent work in other areas related to applied catalysis are also given. © 1999 Elsevier Science B.V. All rights reserved.

Keywords: CO hydrogenation to methanol and ethanol; Formyl intermediate; Dipole–charge interaction with cation; Metal–carboxylic acid; Water–gas shift mechanism; Methane oxidative coupling; Rare-earth catalysts; Composite oxides and oxyfluorides; Active oxygen species; Superoxide ion and active precursor; In situ Raman spectra

1. Introduction

Applied catalysis is among the few branches of applied science that can make tremendous contribution to the international competitiveness of a country. In many industrialised countries, as well as in some developing countries, applied catalysis research and application-oriented fundamental catalysis research are often well integrated, and their intimate interactions have been leading to rapid progress of catalysis science and technology. This paper gives a concise, chronological review of the 40 years of applied catalysis research, along with its interaction with fundamental catalysis research, done at Xiamen University, since 1957 when post-graduate education and research in catalysis at this university were started.

2. Applied catalysis in acetylene and olefin conversion

Before the successful exploitation of Daqing oil field, China was in dire need of basic organic chemicals for the production of synthetic rubber, plastics, and synthetic fibres. In the late 1950s, Xiamen University was in charge of an applied catalysis research project funded by the Ministry of Chemical Industry of China, and in the mid-1960s, in charge of a subproject of the State Key Project no. 29 on application-oriented fundamental catalysis research supported by the State Science and Technology Commission (SSTCC). Our first task was to find a practical catalyst to be used as a substitute for the highly toxic $HgSO_4$–H_2SO_4 catalyst used in acetaldehyde production from carbide-based acetylene. At first, we tried to improve on the co-precipitation-type $(Cd,Ca)_3(PO_4)_2$ catalyst, invented by Gorin [1,2] in USSR, for acetaldehyde

*Corresponding author.

0920-5861/99/$ – see front matter
PII: S0920-5861(99)00004-8

production via vapour-phase hydration of acetylene. By cation exchange of $Ca_3(PO_4)_2$ pellets with $Cd(NO_3)_2$·aq, cation exchange-type $Cd_3(PO_4)_2/Ca_3(PO_4)_2$ catalyst was prepared. Laboratory test and pilot-plant test (fluidised-bed reactor) showed that the $Cd_3(PO_4)_2/Ca_3(PO_4)_2$ catalyst and the similarly prepared $Zn_3(PO_4)_2/Ca_3(PO_4)_2$ catalyst were more active than the corresponding catalyst prepared by co-precipitation method. Chemical analysis and thermometric titration with *n*-butylamine showed that the cation exchange was fast, but practically stopped when Ca^{2+} ions of the surface layer of $Ca_3(PO_4)_2$ pellets were completely exchanged by Cd^{2+} (or Zn^{2+}) ions. Thus much less amount of cadmium was required. But with fluidised-bed reactor, attrition loss of the phosphate catalysts was found to be too serious. Since it was inferred from mechanistic consideration [3] that surface Cd^{2+}, or Zn^{2+} ions were mainly responsible for the catalyst activity, a more robust, more active, and less easily deactivated ZnO/SiO_2 catalyst was prepared from impregnated $Zn(NO_3)_2$ precursor and successfully used as a substitute for the phosphate catalysts. A 400 ton/a pilot-plant test ran smoothly at 643–673 K (370–400°C) for three months in 1973 (with re-activation of the catalyst every five days, or continuously). Space–time yield with the catalyst was ca. 180 g CH_3CHO/l/h (≈81% selectivity) plus ca. 20 g crotonaldehyde/l/h (≈10% selectivity) as a by-product [3]. Subsequently, a small plant was set up to supply the ZnO/SiO_2 catalyst to more than half a dozen small acetic acid plants in China for about five years.

Our second task was to improve on the CrO_x/SiO_2 catalyst developed by the Shanghai Research Institute of Chemical Technology for benzene production via cyclotrimerisation of carbide-based acetylene. The CrO_x/SiO_2 catalyst was found to be highly active and selective, but rapidly deactivated above 413 K, thus excessive amount of cool water was required with practically no way to recover the enormous heat of reaction to produce superheated steam. From mechanistic reasoning and trial experiments, we soon found that Nb_2O_5/SiO_2 catalyst prepared from impregnated oxalate precursor of Nb(V, d^0) was an excellent substitute for the CrO_x/SiO_2 catalyst [4]. A 100 ton/a pilot-plant test of the Nb_2O_5/SiO_2 catalyst at the third Chemical Factory of Xiamen was run very smoothly at 473–523 K for two months, with continuous withdrawal of part of the catalyst for re-activation by carefully burning off very small amounts of non-volatile carbonaceous deposits. With undiluted acetylene, ultra-pure benzene was produced (∼1 kg/kg h). From the observed products distribution in experimental study of HC≡CH and $CH_3C{\equiv}CH$ co-cyclotrimerisation, as well as from the high selectivity and activity, a Diels–Alder type mechanism for the benzene formation was proposed [4], based upon the formation of metallo-cyclopentadiene intermediate, M(HC=CHCH=CH) on coordination-unsaturated Nb(V, d^0) active-site. Note that in this paper, underlined atomic symbols denote surface-bound atoms of adspecies.

The pilot-plant test of Nb_2O_5/SiO_2 catalyst and the small-scaled production of ZnO/SiO_2 catalyst were discontinued (though the two catalytic processes may be documented as two successful reserve technologies for the production of acetaldehyde and benzene from acetylene in case of petroleum shortage) after the successful large-scale exploitation of Daqing oil field. We then re-oriented our catalysis research direction in basic organic synthesis, first to catalysis in ethylene, propylene polymerisation and selective oxidation [5,6] for a few years, then focusing our attention to CO hydrogenation and light alkanes activation and selective oxidative-conversion. In the meantime, chemical modelling of biological nitrogen fixation was also started (including ammonia synthesis over iron-based catalysts).

3. Applied catalysis related to chemical modelling of biological nitrogen fixation

In 1972, a multi-disciplinary research project, ''Chemical modelling of biological nitrogen fixation'' was organised as a state key project, involving many research institutes and universities, and supported by the SSTCC for 10 years. The front line of the project was actually integrated with applied catalysis research on industrial ammonia synthesis catalysts, aimed at finding practical catalysts which could be used under lower temperature and pressure. An electron donor–acceptor (EDA)-type catalyst [7], Fe(II)–phthalocyanin–K–graphite system, was tried by the joint efforts of two universities and two research institutes, as well as a factory. The EDA-type catalyst proved to be very

active even at 573 K. But laboratory and pilot-plant tests failed to produce a catalyst with sufficient stability, conceivably due to high volatility and poison-sensitivity of metallic potassium. However, ammonia synthesis by the EDA-type catalyst conceivably involves N_2 coordination, dissociative chemisorption of H_2, H-spillover via concerted electron and proton transports, and electron storage afforded by the large conjugated system. This is in principle analogous to our concept about the mechanism of nitrogenase catalysis [8], this mechanistic study has led us to further development of the concept of catalysis by coordination activation [9] and to the study of the probable mechanistic relationship between ammonia synthesis catalysed by promoted iron catalysts and by nitrogenase [10,11]. In the experimental study of ammonia synthesis over promoted iron catalysts in our laboratory [12,13], in situ Raman spectroscopy was found to be very useful for the characterisation of chemisorbed species with sufficient polarisability, e.g., N_2, N, NH, and somewhat unexpectedly, H ($H^{\delta-}$ on Fe^0) on the functioning catalyst.

Recently, in rationalisation of chemical modelling of nitrogenase catalysis, a labile-mouthed M-cluster-cage model of the substrate-binding FeMo-cofactor with two proton-transport pathways and mechanisms of shape-selective reduction of nitrogenase substrates have been proposed by Tsai and Wan [14,15]. Besides the theoretical interest of increasing our understanding about the functioning of this key enzyme with its multi-nuclear substrate-binding sites and proton-transport pathways, fundamental study of nitrogenase catalysis has led us to some ideas about catalysis by cluster complexes, and may have practical significance in guiding the design and preparation of catalysts for certain types of reactions; e.g., highly selective hydrogenation of acetylene to ethylene.

4. Metal–metal oxide catalysts for CO hydrogenation to methanol and ethanol

Since the two oil crises in the 1970s, catalysis in C_1 chemistry has become an area of extensive research internationally. In China, a State Key Project of this research subject was organised and supported by the National Natural Science Foundation of China (NNSFC) for five years since 1987. At Xiamen University, one of the research topics was molecular catalysis in CO hydrogenation to methanol (COHTM) over Cu–ZnO-based catalysts and to ethanol (COHTE) over Rh–metal-oxide-based catalysts, aimed at comparing the functions of metal oxide promoters (or cocatalysts) in these two systems, and getting some ideas for catalyst improvement from molecular catalysis approach.

4.1. CO hydrogenation to methanol over Cu–ZnO-based catalysts

For COHTM over Cu–ZnO-based catalysts, it has been generally accepted since the mid-1980s that formyl adspecies is a key intermediate, and that there is pronounced synergy between the copper component and ZnO [16,17]; the nature of this synergy has been a subject of extensive investigation. It is known that the energy barrier for partial hydrogenation of CO to formyl intermediate (H$\underline{\text{C}}$=O) is about 20 kcal/mol [18] (1 kcal=2.1868 kJ). Note that from the handbook [19], the dipole moment of aldehydic carbonyls (2.3–2.7×10^{-18} e.s.u.) is one order of magnitude larger than that of CO (0.10×10^{-18} e.s.u.). It has been postulated by Tsai and co-workers [20,21] that the formation of H$\underline{\text{C}}$O in COHTM over Cu–ZnO-based catalysts may be greatly promoted by dipole–charge interaction of the $Cu^{\delta+}$-bound H$\underline{\text{C}}$=O carbonyl with Zn^{2+}. The magnitude of this interaction energy roughly estimated from classical model, $N\mu(ze)\cos\theta/r^2 \approx N(2.3\times10^{-18})(2\times4.8\times10^{-10})\cos110^\circ/(3.0\times10^{-8})^2$, is about 12 kcal/mol. This also implies that in every subsequent step of the surface reaction, the CO-derived O-end of the adsorbed intermediate will keep interacting or linked with Zn^{2+}, and that the H$\underline{\text{CO}}$ may be readily and successively hydrogenated to $CH_3\underline{\text{O}}$–bound to Zn^{2+}, and finally converted to CH_3OH via protonation (with protonic hydrogen taken from a neighbouring –$\underline{\text{O}}$H), or hydrogenation. This has led to the suggestion of $[Cu^0\underline{\text{H}}]_xCu^{\delta+}OZn(\underline{\text{H}})OH$ active-centre for COHTM [20,21]. In view of the known experimental fact [16,17] that in COHTM over Cu–ZnO-based catalyst, H_2O(g) in small amount acts as a promoter, and in larger amount as an inhibitor; while water–gas shift reaction (WGS) is not inhibited at all by H_2O [16,17], a virtually one-sited active-centre, $Cu^{\delta+}$ at the surface lattice of ZnO and linked with the epitaxy copper, has been suggested by Tsai and

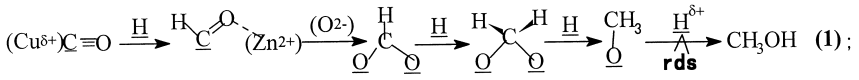

Scheme 1.

co-workers [20,21] for WGS, along with the suggestion that the WGS may involve the usual *cis*-migratory insertion of CO into Cu – OH to form CuC(O)OH. This is *not* a Cu-ligating formate (HCOOCu or HCOOCu via *unusual* insertion of CO into CuO – H), but a metal–carboxylic acid, of which the formation, structure and properties have been well reviewed by Bennett [22], who has mentioned that metal–carboxylic acid might be an intermediate of WGS in homogeneous catalysis. The CuC(O)OH may readily liberate CO_2 to give CuH, followed by H_2 liberation with a neighbouring H. As more information became available in the literature (e.g., formation of bidentate formate intermediate (HCOO−) in COHTM observed from in situ FTIR spectra [23], formation of dioxymethylene (H_2COO−) in COHTM [24], as well as in HCHO adsorption on Cu–$ZnAl_2O_4$ [25], and on Cu/ZrO_2 [26,27], and H-spillover in either direction between copper surface and ZnO [28,29]), it has become possible for Cai et al. [30] to add to the COHTM scheme more details taken from relevant literature. The whole scheme is shown in Scheme 1, the metal–carboxylic acid mechanism for WGS [20,21] is assumed to be still applicable (see Scheme 2).

The role of CO_2 is a key issue in methanol synthesis from syngas over Cu-based catalysts. It is known [16,17] that the rate of COHTM is greatly promoted by a small proportion of CO_2 in the syngas. However, it has since been well illustrated, mainly by the ICI scientists [31,32] that, with more than a few percents of CO_2 in the syngas, CO_2 hydrogenation to methanol (CO_2HTM) with Cu-bound bidentate formate (HCOO) as a key intermediate becomes predominant, with practically complete suppression of COHTM; that under the same operating conditions, catalyst activities for CO_2HTM and WGS both depend only on the surface area of copper, practically irrespective of the supports (ZnO–Al_2O_3, SiO_2, Al_2O_3, MgO, MnO, ZnO); and that during the CO_2HTM reaction in the presence of very little CO, about 40% of the copper surface is covered by oxygen (i.e., about 80% saturation of available sites by N_2O titration [33]). This amount of surface oxygen is determined by titration with CO to give CO_2, followed by liberation of H_2 in an amount corresponding to about one monolayer of H, which is assumed to come mostly from sub-surface H [33]. Though the kinetics and mechanism of CO_2HTM are beyond the scope of this report, it is pertinent to note here that the predominance of CO_2HTM (with bidentate formate as a key intermediate) and the absence of carbon-containing, common intermediate in CO_2HTM and WGS [32,33] may be taken as direct evidence against the formate mechanism for WGS (suggested by many researchers, as seen in some comprehensive reviews [34,35]), but not against the metal–carboxylic acid mechanism and the redox mechanism for WGS, the former mechanism may even be more tenable than the latter, or at least as an alternative of the latter. A considerable fraction of the copper surface may actually be covered by hydroxyls (as also mentioned by Ghiotti and Boccuzzi [35]), rather than by [Cu]-bound oxygen. *Cis*-insertion of CO into $Cu^{\delta+}$–$(OH)^{\delta-}$ anywhere on the copper surface to form Cu – C(O)OH should be able to take place readily, followed by liberation of CO_2 and H_2, as shown in Scheme 2. Thus CO titration cannot differentiate surface O from –OH. However, with metal–

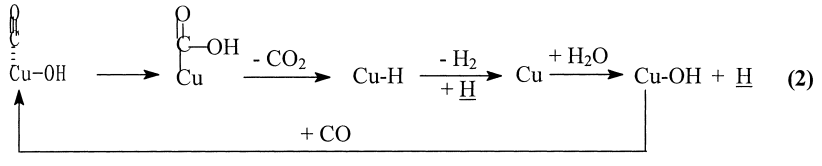

Scheme 2.

carboxylic acid mechanism for WGS, it is not necessary to assume that most of the H_2 liberated may have come from sub-surface H (which may be able to combine readily with surface O to form surface hydroxyls). Moreover, copper with much sub-surface H may not be able to displace H_2 from H_2O fast enough, Cu being less electropositive than H_2. Waugh [33] has remarked that the molecular description of the reaction pathways for CO_2HTM and WGS are still crude. It is desirable to obtain a clearer picture of molecular catalysis in WGS and CO_2HTM on copper-based catalysts. This is also a requisite for setting up reliable kinetic model in process development [36].

More recently, a Cu–ZnO-based catalyst promoted with cerium oxide has been worked out by Yang et al. [37] for methanol synthesis with H_2-rich syngas. The catalyst has been commercialised by the Nanjing Catalyst Factory for use in coproduction of methanol in ammonia synthesis, with improved methanol yield and catalyst stability.

Incidentally, COHTM over Pd–Mg^{2+}/SiO_2 has also been studied by Shen et al. [38–40] for a period of time. Research is now also in progress here in the design and preparation of compatible dual-catalysts system for high conversion methanol synthesis via ''one pot'' reactions of the known, consecutive methyl-formate formation and hydrogenation.

4.2. *CO hydrogenation to ethanol (COHTE) over promoted rhodium catalysts*

In CO hydrogenation to ethanol (COHTE), promoter effects are also observed with metal oxide promoters [41,42]. The catalyst system is a known example of strong metal–support interaction (SMSI) [43], or strong metal–promoter interaction (SMPI), involving Rh and a promoter cation of variable valency and/or strong oxyphilicity, such as $Mn^{(2,3,4)+}$, $Ti^{(3,4)+}$, or Zr^{4+}, Nb^{5+}. Some researchers [44,45] have proposed that the function of the metal oxide promoter is to assist in weakening the C ≡ O bond for direct bond rupture via formation of bridging or tilted CO (a large lowering of ν_{C-O} to 1715 cm^{-1} being taken as an argument), followed by hydrogenation of C to form CH_2, or CH_3 and reaction with CO by *cis*-coupling or *cis*-insertion to form ketene or acetyl as C_2-adspecies. This is called the dissociative mechanism for the formation of CH_3 in the CH_3CH_2OH. However, in the study of CO hydrogenation over Rh/SiO_2 catalyst, Orita et al. [46] have observed an IR band at 1587 cm^{-1}, ascribable to symbol ν_{C-O} of HC=O and observable only in the presence of both CO and H_2 (though the two characteristic ν_{C-H} bands were not observed, probably due to too low concentration of HC=O on Rh/SiO_2). They have also shown by isotopic tracings that the CH_3 groups of the light alkanes side-products and that of CH_3CH_2OH are from the same C_1 intermediate, thus extending the significance of searching for this C_1 species to alkane formation over rhodium catalyst. Many investigators have observed that, over rhodium catalysts, hydrogen-assisted CO dissociation is faster than direct dissociation of CO in the absence of H_2, so they have favoured some form of associative mechanism in which C–O bond rupture in the presence of hydrogen is preceded by partial hydrogenation of CO. Thus Takeuchi and Katzer [47] have proposed a CO–formyl–carbene–ketene mechanism for the major pathway of C_2 formation from CO; they have speculated ketene rearrangement to epoxyethene cyclic intermediate before further hydrogenation to ethanol to account for the observed isotopic scrambling in the ethanol formed, starting with H_2 and $C^{18}O/^{13}CO$. But Deluzarche et al. [48] have pointed out that the observed isotopic scrambling might be accounted for by rapid isotopic exchange of the acetaldehyde intermediate with the H_2O formed in CO hydrogenolysis, without recourse to the speculation of epoxyethene cyclic intermediate. For CO hydrogenation to CH_4 and other alkanes. Riecke and Bell [49,50] have suggested that C–O bond breaking is preceded by partial hydrogenation of CO to H_2CO, and promoted by oxyphilic interaction of the promoter cation with the oxygen-end of H_2CO. Even in CO hydrogenation to CH_4 over Ni/SiO_2, Mori et al. [51] have observed hydrogen-assisted CO dissociation faster than direct dissociation of CO, and deuterium inverse kinetic isotope effect (k_H/k_D=0.75) on the methanation reaction rate. Incidentally, hydrogen-assisted CO dissociation in metal-catalysed CO hydrogenation might be even more general; it has been remarked [52] that, under certain conditions, deuterium inverse kinetic isotope effects of similar magnitude for methanation reaction have been observed with many other group VIII metals, including Fe and Ru.

Based on the literature knowledge about the compositions and properties of the catalyst systems and the

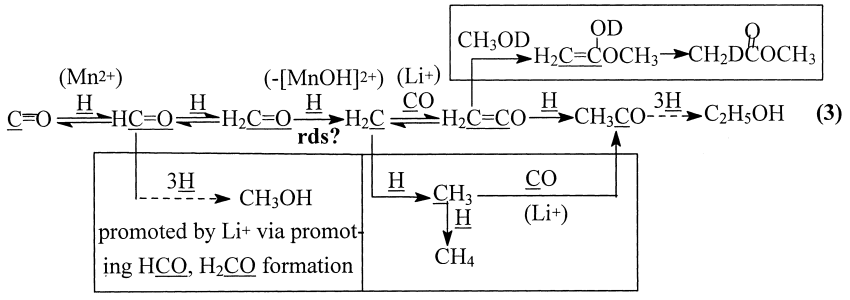

Scheme 3.

product and side products distribution, and by similar reasoning as in the study of promoter action in COHTM, it has been proposed by Tsai and co-workers [53–55] that in COHTE over promoted rhodium catalysts the oxyphilic promoter-cation may also promote HCO formation through dipole–charge interaction, or even through formation of metalloxy-carbene (similar to Bercaw's zirconoxy-carbene [56]); as well as hydrogenolysis of HCO to form Rh-bound $\underline{C}H_2$ and promoter-cation bound –OH, and that this may be followed by the formation of $H_2C{=}C{=}O$ (a π-olefinic–Rh complex [57]) promoted by dipole–charge interaction with Li^+ and successive hydrogenation to ethanol. (Li^+, better than Na^+ and K^+, can also effectively catalyse COHTM over rhodium, most probably by dipole–charge interaction of the HC=O with Li^+, and probably also of $H_2C{=}O$ carbonyls with Li^+.) This may occur before the removal of the –OH from the promoter cation (e.g., Mn^{3+}) by hydrogenation, to account for the high C_2 selectivity. Thus a scheme of the main pathway of COHTE have been suggested, as shown in the central part of Scheme 3, i.e., a scheme of CO–formyl–carbene–ketene–acetyl–(acetaldehyde, or CH_3COH)–ethanol pathway, and the systematic examination and establishment of this scheme have been set out by a combination of various methods. The framed blocks in Scheme 3 show the chemical trapping of ketene with CH_3OD (likewise, for MeAc side-product formation), and side-reactions for methanol and methane formation.

First of all it is essential to detect and determine the formyl adspecies. Following the method of Deluzarche et al. [58], Wang et al. [59,60] used CH_3I in excess as chemical trapping agent for trapping the formyl intermediate, DC=O, in ethanol synthesis from CO–$2D_2$ (isotope purity $\geq$99.9%) over Rh–MnO/SiO_2 catalyst, and found quite unexpectedly from the GC–MS mass spectrogram of the acetaldehyde fraction slightly stronger signals of mass 29 (HCO) and mass 44 (CH_3CHO) than that of the expected mass 30 (DCO) and mass 45 (CH_3CDO) (Fig. 1A). It appeared

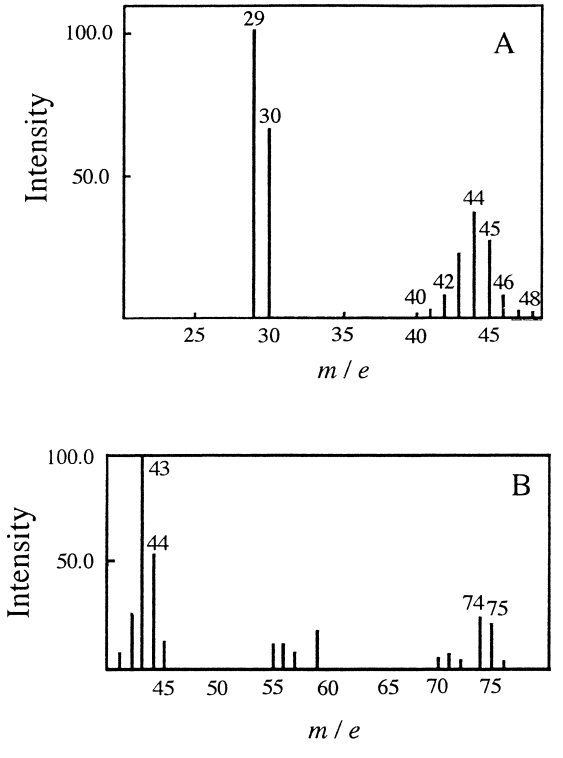

Fig. 1. A: GC–MS pattern of acetaldehyde fraction from chemical trapping with CH_3I of DCO in CO+$2D_2$ reaction over Rh/MnO_x/SiO_2 at 493 K, 0.1 MPa. B: GC–MS pattern of methylacetate fraction from in situ chemical-trapping of $H_2C{=}C{=}O$ with CH_3OD added into CO–H_2 (2:1) over Rh/MnO_x/Li^+/SiO_2 at 493 K, 0.1 MPa.

that some of the trapping agent had dissociated at the CH_3 group on rhodium surface to give H, which was trapped in some way (either by CH_3CO, or successively by CO and CH_3) to give CH_3CHO. Since there were considerable amounts of CO and D besides DCO on the working rhodium catalyst before the excess CH_3I was injected onto it, the possibility that CH_3I, besides trapping DCO, might also trap considerable amount of the CO and D successively to give CH_3CDO, must be taken into consideration. Considering that DCO is directly bound to Rh and also held by the promoter cation Mn^{2+} through strong dipole–charge interaction, while D and CO (the dipole moment of which is probably one order of magnitude smaller than that of DCO) are more weakly bound to the surface, a slight modification of the chemical trapping method has been made by Wang et al. [59,60]: by sweeping the catalyst bed with a stream of N_2 for varying periods of time (0, 3, 5, 13 min) after the reaction and before the injection of excess CH_3I, it was found that after 3 min of sweeping with N_2, the amount of DCO (probably along with small amounts of CO and D) trapped by CH_3I to form CH_3CDO decreased by only 50% while the amount of surface D decreased by about 96%. The results showed that DCO intermediate was actually formed in COHTE, and more tightly bound at the catalyst surface than D (and CO).

Conceivably, the active centre of COHTE on promoted rhodium catalysts must be situated at the metal–promoter boundary, as suggested by many investigators. Du et al. [61] have substantiated this point by their studies of silica-supported rhodium catalysts promoted separately with various rare-earth oxides. They have demonstrated that the metal–promoter interaction and promoter effect are both more pronounced with rare-earth oxides of variable cationic valency than with those of stable cationic valency. The strong metal–promoter interaction has been illustrated by Hu and Wang [62] with quantum-chemical calculations (DV-Xα-SCC method), using a Rh_4OMnO cluster model suggested by Wan. A section in a review by Hindermann et al. [63] provides valuable reference for CO adsorption.

More information about formyl intermediate in COHTE over Rh–MnO/SiO_2 catalyst, together with relative activities of the linear and bridging CO, or tilted CO, has been obtained by Wang et al. [59,64]

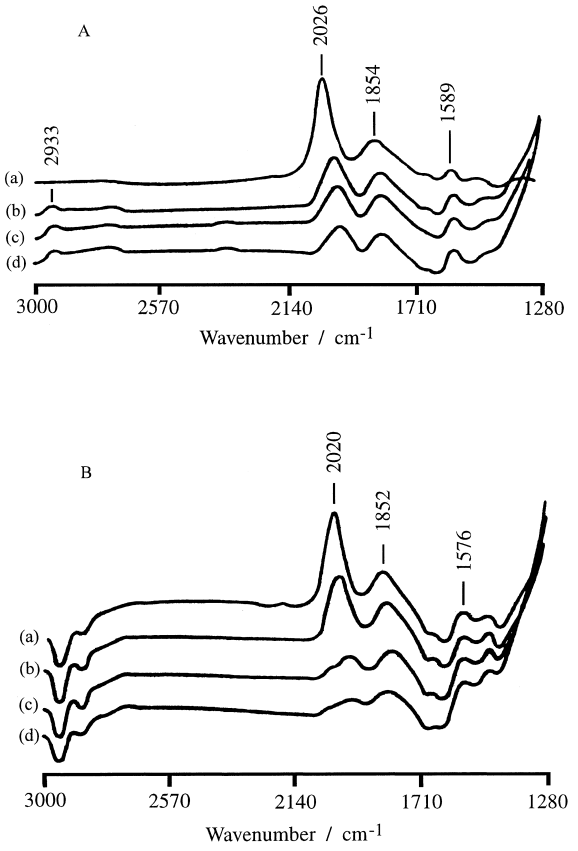

Fig. 2. TPSR–FTIR of pre-adsorbed CO on $Rh/MnO_x/SiO_2$ with flowing A: H_2, and B: D_2, at (a) 328, (b) 428, (c) 463, and (d) 493 K.

from temperature-programmed surface reaction (TPSR)–FTIR study of pre-adsorbed CO on Rh–MnO/SiO_2 with H_2 flow and with D_2 flow. The characteristic ν_{C-O} IR bands of HCO (1589 cm^{-1}, very close to that observed in this laboratory by Fu et al. [65] at 1591 cm^{-1}, by slow displacement and reaction of pre-adsorbed H on Rh–MnO/SiO_2 with CO at 503 K, the HCO characteristic ν_{C-H} at 2708 and 2659 cm^{-1} also being observed) and DCO (1576 cm^{-1}) were clearly observed and identified by the frequency red-shift (∼13 cm^{-1}) of ν_{C-O} due to the secondary isotope effect of D. This is comparable with the ν_{C-O} red-shift (9 cm^{-1}) from ν_{C-O} of HCO at 1520 cm^{-1} to ν_{C-O} of DCO at 1512 cm^{-1} on Cu–$ZnAl_2O_4$ observed by Lavalley et al. [24]. Note that, as seen from Fig. 2, the intensity of the ν_{C-O} IR band (at 2020 cm^{-1}) of linear CO decreased conspicu-

ously faster with temperature programming than that (at 1852 cm^{-1}) of bridging $\underline{C}O$, especially from Fig. 2B $\underline{C}O + D2$, due to the deuterium inverse kinetic isotope effects on COHTE and COHTM (these two reactions have slightly different deuterium inverse kinetic isotope effects [66] and different activation energies [67]). This may be taken as direct evidence [68] showing that linear $\underline{C}O$ is in fact more reactive in COHTE and COHTM than the bridging or tilted $\underline{C}O$, in spite of the considerably lower ν_{C-O} of the latter than that of linear $\underline{C}O$. Direct evidence has also been reported by Chuang [69,70] for much faster hydrogenation and *cis*-insertion of linear $\underline{C}O$ than bridging or tilted $\underline{C}O$. This is in line with the proposal [9,21,53–55] that the promoter acts to lower the activation energy of the reaction by partial stabilisation of the highly unstable intermediate, rather than by binding the reactant molecule more tightly to weaken the bond to be broken (unless direct bond rupture happens to be the rds). This is reminiscent of Pauling's famous remark that enzymes bind the transition states of reactions, while antibodies bind the ground states of the substrates.

To examine the C_2 formation pathway, Liu et al. [54,55] have carried out in situ chemical trapping of the expected $H_2\underline{C}{=}\underline{C}O$ and $CH_3\underline{C}O$ with CH_3OD to form $CH_2DCOOCH_3$ and CH_3COOCH_3, respectively, and shown that the mol% of $CH_2DCOOCH_3$ in the methyl acetate fraction (determined by GC–MS) (Fig. 1B) can be greatly increased by increasing the CH_3OD/H_2 ratios in the feed, the result indicates the presence of ketene and acetyl intermediates in comparable quantities; and in situ chemical trapping of ketene being strongly competed by its further hydrogenation. It is inferred that ketene, rather than $\underline{C}H_3$, is the major precursor of $CH_3\underline{C}O$.

Lastly, to account for the isotopic scrambling in the ethanol obtained from hydrogenation of $C^{18}O$–^{13}CO (1:1) observed by Takeuchi and Katzer [47], in situ chemical trapping of ketene and acetyl intermediates with oxygen isotopic-exchange has been carried out by Wang et al. [59,71] by adding varying amounts (ca. 5–15 mol% of the feed) of $D_2^{18}O$ into the feed CO/nH_2 (n=1, 2, 3) over $Rh/TiO_2/SiO_2$ catalyst at 493 K, 0.1 MPa, and collected the organic compounds (along with the co-produced water) in the reactor effluent in liquid-nitrogen cold trap, and also recovered the ketene, acetyl, and acetate adspecies on the catalyst surface in the forms of four methyl esters (one unlabelled, one doubly labelled, and two singly labelled with $^{18}O/^{2}H$) by thoroughly purging the organic adspecies from the catalyst bed with a stream of CH_3OH-containing N_2. It was found that the mol% of ^{18}O-labelled esters was 2–3 times larger than that of mono-deuterated acetate in each case of the $CO/H_2/D_2{}^{18}O$ ratios, indicating that the reversible hydration and dehydration of $H_2\underline{C}{=}\underline{C}{=}O$ with non-ligating carbonyl–O were considerably faster than the rearrangement of the hydrated ketene, $H_2\underline{C}{=}\underline{C}$ (^{18}OD) (^{16}OD), to mono-deuterated acetic acid. In a blank test, ethanol showed practically no ^{18}O isotopic-exchange with $H_2^{18}O$. Statistical calculations [59,71] demonstrated that two rounds of ketene hydration–dehydration reactions with the H_2O co-produced in COHTE are nearly enough to account for the isotopic scrambling observed by Takeuchi and Katzer [47]. Some contribution to the observed isotopic scrambling must have come from reversible hydration and dehydration of the acetyl and acetaldehyde intermediates.

Thus the proposed scheme for the main reaction pathway of COHTE over promoted rhodium catalysts has been verified in some detail [59,60,64,72]. The results show that partial hydrogenation of $\underline{C}O$ to $H\underline{C}O$ promoted by strong dipole–charge interaction with oxyphilic cation followed by hydrogenolysis of $H\underline{C}O$ to $\underline{C}H_2$ is energetically more effective than direct cleavage of the very strong CO bond promoted by multi-nuclear coordination of $\underline{C}O$ (which in fact seriously retards *cis*-insertion of $\underline{C}O$ [69,70]). This is mainly due to the much larger carbonyl dipole moment and O-end nucleophilicity of $H\underline{C}{=}O$ than that of $\underline{C}O$. This may have more general significance in fundamental and applied catalysis in CO hydrogenation.

5. Rare-earth-based catalysts for OCM and oxidative dehydrogenation of light alkanes

Oxidative coupling of methane (OCM) to ethane and ethylene [73] over reducible or irreducible metal oxides-containing catalysts with cyclic (redox)-feed [73] or cofeed [74] mode of operation has attracted great, world-wide interest for its potentiality to be developed into a ''smart process'' for utilising the enormous, global natural-gas resources. It is generally

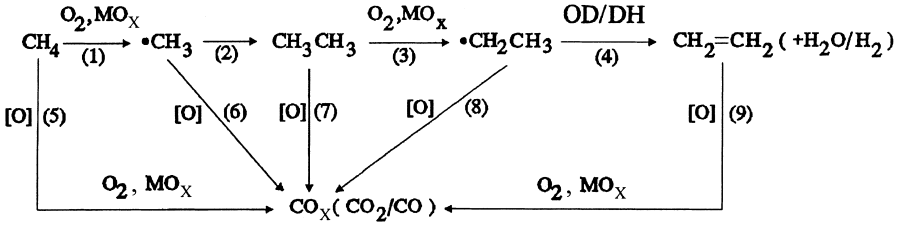

MO_X= composite metal oxide , OD = oxidative dehydrogenation , DH = dehydrogenation

B.E.	$H\text{-}C_2H_5$	<	$H\text{-}CH_3$	<	$H\text{-}CH{=}CH_2$	≤	$H\text{-}CH_2\bullet$;	H-OH	H-OOH
kcal	100 (98)		105		≥108		110	≥110	87

Fig. 3. Schematic diagram of OCM reactions and major side-reactions (over irreducible rare-earth-based composite oxides).

accepted, as seen from many review articles (e.g., [75–78]), that OCM involves a series of complex heterogeneous–homogeneous free radical reactions, initiated by H-abstraction from CH_4 by surface active-oxygen species to liberate CH_3 radicals, which couple in the gas phase to give C_2H_6 as the primary product, along with coproduced H_2O. Ethylene appears to be a secondary product formed via oxidative dehydrogenation of ethane at the catalyst surface, and via free radical hydrogen-transfer reaction in the gas phase, and probably in minor amount by thermal dehydrogenation at the high temperature of OCM. All of the hydrocarbons may undergo deep oxidation to CO_2 and CO at the catalyst surface, or in the gas phase in the presence of O_2. A diagrammatic sketch of the reaction intermediates, products, and major side-products formation is shown in Fig. 3.

It is also known that OCM catalysts with stable cationic valency can only be used in cofeed operation and show practically no activity with methane in the absence of O_2 [75–79], while those with variable cationic valency can be used in both cofeed and cyclic-feed operations. With irreducible OCM catalysts, lattice O^{2-} ions associated with cations of stable valency are obviously inactive towards methane, and certain active oxygen-adspecies must be there to initiate the OCM reaction via H-abstraction from CH_4 to form CH_3. Adsorption of O_2 on metal oxides with stable cationic valency may lead to the formation of a variety of oxygen adspecies, such as $\underline{O}_2$, $\underline{O}_2^-$, $\underline{O}_2^{2-}$, and $\underline{O}^-$; by stepwise transfer of 1–2 electrons to $\underline{O}_2$ from 1–2 lattice O^{2-} ions; with concomitant reduction of 1–2 O^{2-} to 1–2 $\underline{O}^-$, which may also be formed from dissociation of $\underline{O}_2^{2-}$. Further transfer of an electron from O^{2-} to $\underline{O}^-$ produces no new species, only an exchange of sites; namely, hole migration. This is further complicated by the possibility that O_2 (or $\underline{O}_2$) may incorporate $\underline{O}^-$ (or O^{2-}) to form $\underline{O}_3^-$ (or $\underline{O}_3^{2-}$). In the literature, each of the anionic-oxygen adspecies $\underline{O}^-$, $\underline{O}_2^-$, $\underline{O}_2^{2-}$, and $\underline{O}_3^-$ has been suggested [75–78] to be the principal oxygen-adspecies for OCM, and no unified view has been reached.

With supported or composite metal oxides containing cations of variable valency, cations in the reduced state can readily donate electrons to each $\underline{O}_2$, most probably one by one into the antibonding orbitals of $\underline{O}_2$ to form similar sequence of the diatomic precursors as intermediates, finally, reduce it into two O^{2-}, rather than via direct rupture of the strong O=O double-bond followed by reduction to two O^{2-}. Each of the lattice O^{2-} associated with cations in the oxidised state might have partial radical-anion character (especially those O^{2-} at the surface lattice), and should be able to abstract a H from CH_4, forming CH_3 and $\underline{OH}^-$, aided by concomitant abstraction of an electron from O^{2-} by a neighbouring cation in the oxidised state. However, under certain conditions, the transient precursors $\underline{O}_2^{2-}$, $\underline{O}^-$, and even $\underline{O}_2^-$ (as to be shown later) might also have some chance to react with CH_4 and other hydrocarbons.

In China, research on catalysis in OCM was a part of the State Key Project "Catalysis in C_1 chemistry" supported by the NNSFC for five years and carried over in 1992, along with oxidative dehydrogenation of

light alkanes, into the State Key Project "Catalysis fundamentals in rational utilisation of fossil fuels resources". Research related to OCM has also been carried out in some laboratories supported by other sources of funding.

At Xiamen University and SKLPCSS, studies of irreducible OCM catalysts ($La_2O_3/BaCO_3$ and $K^+/BaCO_3$) were started in 1987 [80]. Since 1990, attention has been focused on REO–AEO-based irreducible composite oxides of the host–dopant type as OCM catalysts [81–87], especially those with defective fluoride structure (DFS) [88,89], because of their very high activity, high selectivity, wide range of anionic-vacancy adjustability, outstanding thermal stability and long life. Novel fluoride-containing REO(F)–AEO(F) catalysts for OCM, as well as oxidative dehydrogenation of ethane and propane (ODE and ODP), have been systematically studied by Wan et al. [90–98] since 1992. In OCM and ODE studies, laser Raman spectroscopy (complemented with FTIR spectroscopy) was found to be very useful for in situ and ex situ characterisation of oxygen-containing surface species.

5.1. *Study of REO–AEO composite oxide catalysts with stable cationic valency*

In the study of OCM catalysts, Liu et al. [81,82] have found that with La_2O_3-based catalysts promoted separately with alkali and alkaline earth cations as dopants, the C_2 selectivity appeared to increase with increasing tendency of the dopant cations to form superoxides and peroxides. However, the promoter actions of Na^+, K^+, Rb^+, and Cs^+ rapidly declined, probably due to formation of stable carbonates (of Na^+ or K^+) or stable hydroxides.

As a prelude to in situ spectroscopic characterisation, Fig. 4 illustrates some information obtainable from ex situ spectroscopic characterisation of adsorbed species on metal oxides.

From Fig. 4A and B it can be seen that, in the room-temperature (r.t.), ex situ laser Raman spectra of oxygen-containing surface-species on samples of metal oxides after various treatments, the Raman bands of the Ba^{2+}-bound $\underline{O}_2^{2-}$, $\underline{O}_2^-$, and $C\underline{O}_3^{2-}$, and of the La^{3+}-bound $C\underline{O}_3^{2-}$ surface species are all well-resolved and characteristic [81,82]. The Raman bands of the surface $C\underline{O}_3^{2-}$ resemble that of unidentate-carbonato ligands in metal complexes [99]. In fact, the Raman spectroscopic features foretell the feasibility of characterising oxygen-containing surface species on metal oxide catalysts by in situ Raman spectroscopy.

It may be inferred from the relative intensities of the Raman signals of $\underline{O}_2^{2-}$ and $\underline{O}_2$ in Fig. 4A(a) versus in A(b) that $\underline{O}_2^{2-}$ is considerably more reactive than $\underline{O}_2^-$ towards CO_2 [82].

Fig. 4C(a) shows the r.t. laser Raman spectrum obtained by Liu et al. [81] of a 10 mol% CsOH/La_2O_3 catalyst freshly activated in air at 973 K, then quenched to r.t. Besides a strong, La^{3+}-bound surface-carbonate band at 1086 cm^{-1} (s) and some un-identified, overlapping weak bands at 1030–1060 cm^{-1}, the Raman signals (r.t.) at 1118 (w) and 800 cm^{-1} (w) were ascribable, respectively, to $\underline{O}_2^-$ and $\underline{O}_2^{2-}$. The disappearance of these two signals from partially deactivated sample C(b) after 3 h on stream of CH_4–O_2–N_2 feed at 973 K, then quenched to r.t. gave some indication that both $\underline{O}_2^-$ and $\underline{O}_2^{2-}$ might exist at 973 K and both might be active-oxygen species towards CH_4.

By the high-temperature–low-pressure–interdiffusion–rapid-quenching–EPR method of Osada et al. [100] for the characterisation of $\underline{O}_2^-$ on an oxide catalyst, Liu et al. [81,82] have shown that $\underline{O}_2^-$ might exist at 1023 K and 16 kPa O_2 on La_2O_3–ThO_2 (La:Th=3:7, single-phase with DFS confirmed by XRD) since inter-diffusion of CH_4 (16 kPa) into the cell with 16 kPa O_2, for 18 min caused the characteristic EPR signal (taken with the quenched sample at 77 K) to disappear, while similar inter-diffusion of N_2 (16 kPa) into the cell with 16 kPa of O_2 at 1023 K for 18 min produced not much change in the intensity of the $\underline{O}_2^-$ EPR signal (at 77 K) (Fig. 4D(a)–(c)). In this way, Osada et al. [100] have previously shown that $\underline{O}_2^-$ might exist on Y_2O_3/CaO catalyst and might be reactive towards CH_4 at 1023 K. Similarly, Yang et al. [101] have shown that $\underline{O}_2^-$ might exist at 1053 K and 13.3 kPa O_2 on a La_2O_3/CaO (10 wt%) catalyst even in the presence of some CO_2, and might be reactive towards CH_4 at 1053 K. However, with similar ex situ EPR method, Louis et al. [102] have found no such reactivity of $\underline{O}_2^-$ on undoped La_2O_3, or $(LaO)_2(O, CO_3)$ catalyst with CH_4. The $\underline{O}_2^-$ adspecies was found to be easily displaced from the sample by CO_2. The different behaviours of doped and

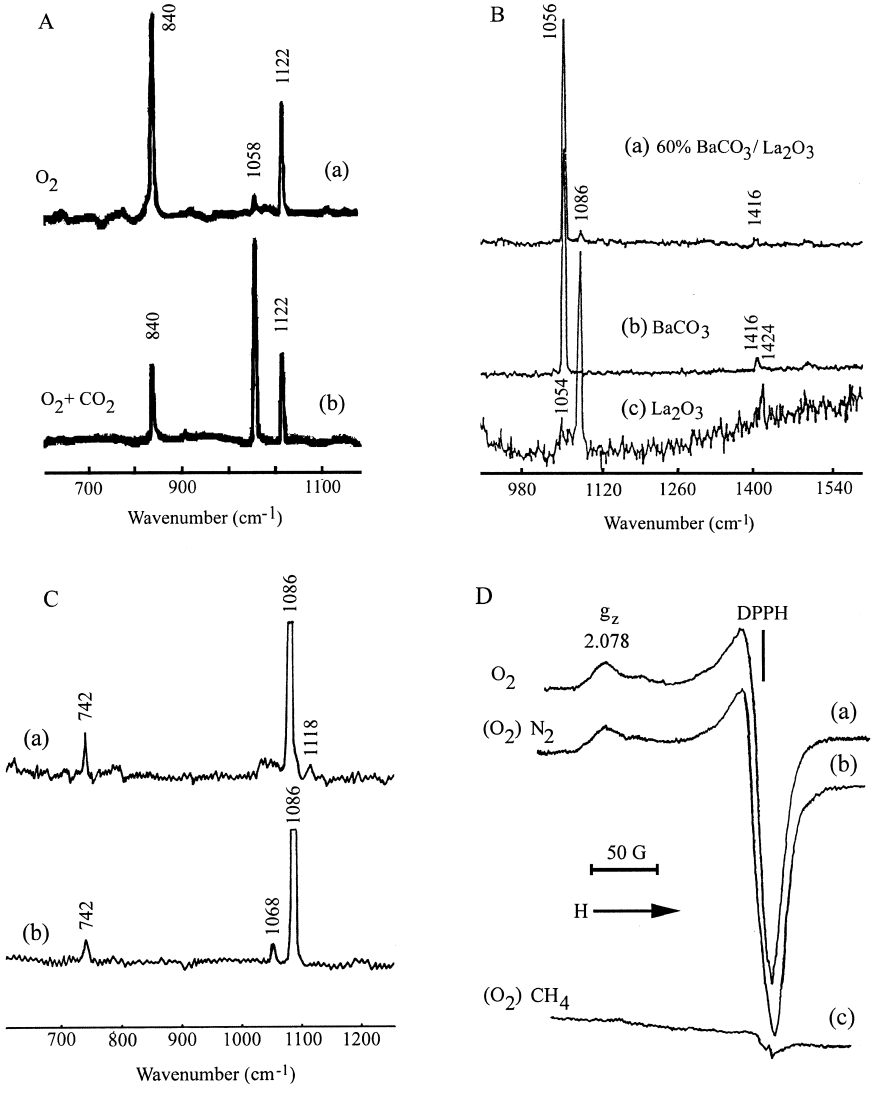

Fig. 4. Ex situ spectra of oxygen-containing species on/in various metal oxides. A: Raman spectra (r.t.) of $BaO_2/Ba(O_2)_2$ quenched to r.t. after heating from 303 to 973 K for 40 min, (a) in O_2 stream versus (b) in O_2–CO_2 (74:26) stream. B: Raman spectra (r.t.) of (a) coprecipitated $La_2O_3/BaCO_3$ (Ba:La=6:4, ignited in air at 1123 K for 5 h, then quenched to r.t.); (b) and (c) reference samples of $BaCO_3$ and La_2O_3. C: Raman spectra (r.t.) of 10 mol% $CsOH/La_2O_3$ catalyst (a) freshly activated by heating in air at 973 K; (b) same catalyst after 3 h on stream of CH_4–O_2–N_2 feed at 973 K. D: EPR spectra (77 K) of uni-phasic La_2O_3–ThO_2 (La:Th=3:7, ignited) quenched to 77 K after separate treatments at 1023 K: (a) heating in O_2 (0.1 MPa, 0.5 h, in EPR cell), evacuation (<0.013 kPa, 1 h), heating in O_2 (16 kPa, 18 min), showing EPR signal of $\underline{O_2^-}$; (b) diffusion of N_2 (16 kPa, 18 min) into (a); (c) diffusion of CH_4 (16 kPa, 18 min) into (a).

undoped $(LaO)_2(O, CO_3)$ is a matter for further investigation.

Much more valuable information about active-oxygen species under OCM reaction conditions can be obtained from in situ Raman spectroscopy. For this purpose, a quartz tubular (4 mm i.d.) Raman cell (and micro-reactor) capable of oscillating vertically up and down has been designed by Liao et al. [103] for scanning around the hot spot of the sample.

With a single-phase Th–La–O_x (Th:La=70:30) OCM catalyst (DFS, confirmed by powders XRD) on stream of CH_4–O_2 (4:1) feed at (a) 953, (b)

1013, (c) 1073, and (d) 1133 K, in situ Raman spectra have been obtained by Liu et al. [84] with bands at 1140 cm^{-1} (mw to w, decreased with increasing temperature) ascribable to ν_{O-O} of $\underline{O_2^-}$ (Fig. 5B(a)–(d)), along with surface carbonate band around 1060 cm^{-1} (vs). When the CH_4–O_2 (4:1) flow was switched to pure O_2 flow over the same Th–La–O_x catalyst at 1013 K, no Raman signal for $\underline{O_2^-}$ was observed (Fig. 5A(a)).

It has been found by Cai et al. [86] that, with a sample of $(LaO)_2(O,CO_3)/BaCO_3$ (La:Ba=2:8, prepared by coprecipitation and ignition) OCM catalyst after 10 h on stream of pure O_2 at 973 K, Raman signals of surface-carbonate at 1052 cm^{-1} (vs) and of $\underline{O_2^{2-}}$ around 810 cm^{-1} (w and broad) were observed, but no Raman signal of $\underline{O_2^-}$ (Fig. 6A(a)). Upon switching the O_2 flow to a flow of CH_4, the Raman signal around 810 cm^{-1} (w) disappeared right away, only the surface-carbonate signal at 1052 cm^{-1} (vs) remained (Fig. 6A(b)). One hour after switching the CH_4 flow to a stream of CH_4–O_2–He (24:6:70, v/v) feed, two more surface-carbonate Raman bands at 1080 (s) and 740 cm^{-1} (wm) appeared, along with a very weak band around 1120 cm^{-1}, which might be $\underline{O_2^-}$ signal, but too weak to be sure (Fig. 6A(c)). With a similarly prepared OCM catalyst La–Ca–O/CaO/(Ba,Ca)CO_3 (La:Ca:Ba=2:4:4) after 10 h in a flow of pure O_2 at 973 K, 0.1 MPa, only the Raman signal at 1052 cm^{-1} (s) of surface-carbonate was observed (Fig. 6B(a)). After switching the O_2 flow to a stream of the CH_4–O_2–He feed and reacting for 20 min at 973 K, a Raman signal at 1140 cm^{-1} (w) ascribed to $\underline{O_2^-}$ was clearly observable, along with a second surface-carbonate signal at 1076 cm^{-1} (m), besides the first one at 1052 cm^{-1} (s) (Fig. 6B(b)). After 20 min more on stream of the feed, the $\underline{O_2^-}$ signal shifted to 1136 cm^{-1} (w), still clearly observable; and the surface-carbonate signal at 1076 cm^{-1} (s) grew in intensity at the expense of the carbonate signal at 1052 cm^{-1} (ms) (Fig. 6B(c)).

In situ Raman spectra of Th–La–$O_x/BaCO_3$ catalyst (Fig. 5C) in flowing CH_4–O_2 (4:1) at 1013 K and 2.0×10^4 h^{-1} GHSV have been obtained by Zhang et al. [85], with Raman band at 1056 cm^{-1} (vs) due to surface carbonate, two bands at 1120 (mw) and 1148 cm^{-1} (mw), and two more bands at 812 (w) and 820 cm^{-1} (w), ascribable to ν_{O-O} of two $\underline{O_2^-}$ and two $\underline{O_2^{2-}}$ adspecies, respectively, in different micro-

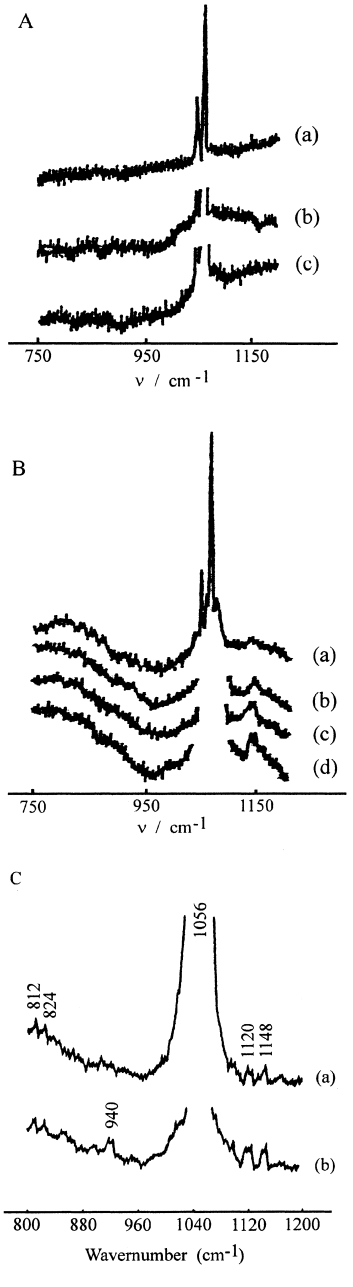

Fig. 5. In situ Raman spectra of A: uni-phasic La_2O_3–ThO_2, 1 h after switching gas flow from CH_4–O_2 (4:1) feed to flowing (a) O_2, (b) CO_2, and (c) CO_2–H_2O (92:8), all at 1013 K; B: functioning La_2O_3–ThO_2 catalyst in flowing CH_4–O_2 (4:1) at (a) 1133, (b) 1073, (c) 1013, and (d) 953 K [84]. C: functioning Th–La–O/$BaCO_3$ catalyst on stream of CH_4–O_2 (4:1) feed at (a) 1013 K, showing $\underline{O_2^-}$ signals at 1120 (w to wm) and 1148 cm^{-1} (w), besides carbonate signal at 1056 cm^{-1} (vs) and two $\underline{O_2^{2-}}$ signals at 812 and 824 cm^{-1} (w); and (b) 773 K, showing a new signal at 940 cm^{-1} (wm) besides the signals in (a) [85].

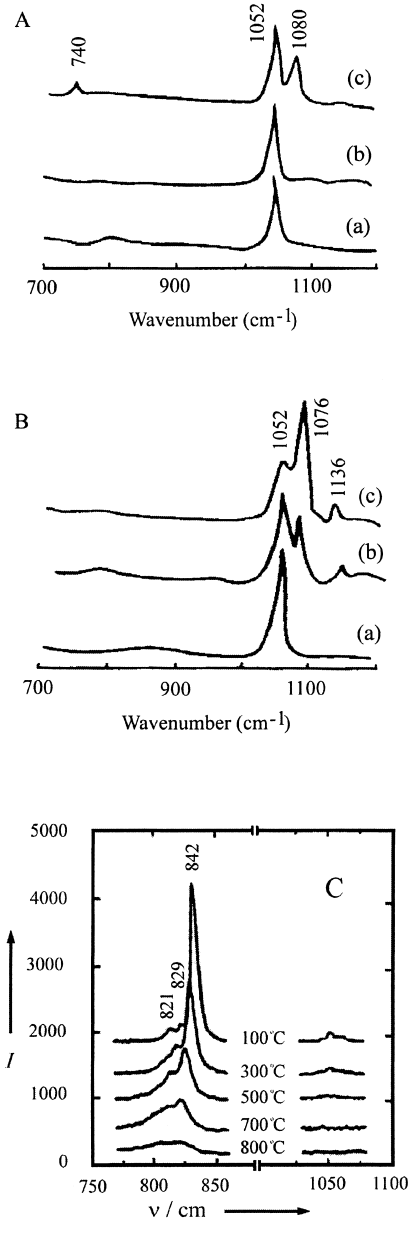

Fig. 6. In situ Raman spectra of OCM catalysts at 0.1 MPa under various reaction conditions. A: $(LaO)_2(O,CO_3)/BaCO_3$ (La:Ba=2:8, ignited) after (a) 10 h on stream of O_2 at 973 K; (b) ca. 10 s after exposing (a) to flowing CH_4 at 973 K; (c) 1 h after swtching the CH_4 flow to flowing CH_4–O_2–He feed at 973 K. B: $(LaO)_2(O,CO_3)/CaO/(Ca,Ba)CO_3$ (La:Ba:Ca=2:4:4) catalyst after (a) 10 h on stream of O_2 at 973 K; (b) after switching the O_2 flow to the feed stream at 973 K and reacting for 20 min; and (c) after reacting for 40 min at 973 K [86]. C (reproduced from [106]): 0.5 mol% BaO/MgO, in O_2 flow at 373–1073 K, showing $\underline{O}_2^{2-}$ Raman signal, and carbonate signal.

environments. Note that the existence of sub-surface $\underline{O}^-$ and $\underline{O}_2^-$ have been shown by Che and coworkers [102,104] by means of EPR method. At lower temperature, the Raman bands of the two superoxide adspecies conspicuously increased in intensity, and at 773 K, an additional Raman band at 940 cm^{-1} (mw) appeared. This band disappeared at temperature only slightly above 773 K. Note that the unidentified species with Raman signal at 940 cm^{-1} (mw) is in the roughly estimated frequency range of $\nu_{1(O–O)}$ stretching of an expected angular species $\underline{O}_3^{2-}$, as active precursor of $\underline{O}_2^-$, as discussed in Section 5.2. A species with Raman signal at 948 cm^{-1} (m–w) on fluoride-containing sample observable in helium flow and in C_2H_6 flow up to 673 and 573 K, respectively, will be shown in Section 5.2.

Note that in situ Raman spectra of La_2O_3, Na^+/La_2O_3, and Sr^{2+}/La_2O_3 in O_2 atmosphere at 973 K have been reported by Mestl et al. [105]. Over La_2O_3, a band at 863 cm^{-1} was observed and ascribed to $\nu_{O–O}$ of O_2^{2-}. After the O_2 flow was switched to a flow of CH_4, the Raman band gradually decreased in intensity, shifted to 813 cm^{-1}, and finally disappeared. After switching the CH_4 flow to a flow of CH_4–O_2, the 863 cm^{-1} band reappeared. Unfortunately, the observation of the 863 cm^{-1} Raman signal was not very reproducible according to Lunsford [75]. In situ Raman spectra of 0.5 mol% BaO/MgO in a flow of O_2 at 373–1073 K have been reported by Lunsford et al. [106], with a major Raman band at 842–829 cm^{-1}, ascribable to $\underline{O}_2^{2-}$, and a band at 1050 cm^{-1} (w) due to surface carbonate (Fig. 6C), but no $\underline{O}_2^-$ signal in CH_4 and O_2 flow under OCM working conditions, only a strong carbonate signal was observed. Note that the absence of $\underline{O}_2^-$ Raman signal in O_2 atmosphere is no longer a surprise. However, the Ba^{2+}/MgO is quite different from the alien-valence host–dopant composite-oxides system with comparable cationic radii, so the behaviours might be different. It would be interesting to examine the presence or absence of $\underline{O}_2^-$ Raman signal around 1115–1165 cm^{-1} with the Sr^{2+}/La_2O_3 catalyst under OCM cofeed-operation conditions.

The in situ Raman spectra obtained with La_2O_3–ThO_2 uniphasic catalyst and La–Ca–O/CaO/$(Ba,Ca)CO_3$ multi-phasic catalyst under OCM cofeed conditions versus in pure O_2 stream reviewed above definitely confirm that $\underline{O}_2^-$ adspecies can exist on the

rare-earth-based composite oxides under OCM cofeed reaction conditions in the presence of large amounts of surface-carbonates and considerable concentration of CO_2 in the gas phase (contrary to the suggestion by some authors [107,108] that the formation of $\underline{O}_2^-$ adspecies might be sensitive to the inhibition by surface carbonates and CO_2), and up to very high temperature (e.g., 1133 K), much higher than the decomposition temperatures of $Ba(O_2)_2$, KO_2, and CsO_2 (contrary to the suggestion by some authors [109,110] that $\underline{O}_2^-$ might be too unstable to exist at the high temperature of OCM). Evidently, the high-temperature stability of $\underline{O}_2^-$ is due to additional stabilisation of the $\underline{O}_2^-$ adspecies by the surface crystal-field, with reference to the energy diagram of various oxygen species (O^{2-}, O_2^{2-}, O^-, O_2^-, O_2) in the gas phase, in the solid phase, and in the surface of a binary oxide given in a review by Bielanski and Haber [111]. Conceivably, the crystal-field at a surface-lattice anionic site of rare-earth dioxide (REO_2) or sesquioxide (Ln_2O_3) is considerably stronger than that of the alkali oxides and AEO.

With the existence and reactivity of $\underline{O}_2^-$ observed at high temperature, Liu et al. [82,83] have been able to advance several arguments in favour of $\underline{O}_2^-$ being the active-oxygen adspecies with higher OCM selectivity than $\underline{O}_2^{2-}$: (1) The OCM selectivity of many catalyst systems is known to increase with increasing temperature in the range 923–1073 K, while $\underline{O}_2^{2-}$ may be reactive towards CH_4 at much lower temperature as indicated by the reactivity of metal peroxides [109,110]. (2) From the relevant bond energies listed as an appendix under Fig. 3, H-abstraction from CH_4 by $\underline{O}_2^-$ may be endothermic by about 18 kcal/mol (while that by $\underline{O}^-$ may be exothermic by several kcal/mol); this is a reaction step of breaking a stronger bond and forming a weaker bond, so deuterium normal kinetic isotope effect, $k_H/k_D>1$, for this step may be expected from zero-point energy consideration; and deuterium normal kinetic isotope effect has been observed for OCM under usual OCM reaction conditions [77], though the rate-determining step of OCM may change under other conditions [75]. (3) It is known that CO_2 can exert significant promotional effect on OCM selectivity, probably by virtue of inhibiting the less selective active-sites [75]; and that CO_2 can react very fast with $\underline{O}_2^{2-}$, in fact, considerably faster than $\underline{O}_2^-$, according to the observation of Liu et al. [82]; as shown in Fig. 4A(a) versus (b); this again indicates that $\underline{O}_2^{2-}$ is less likely to be an oxygen-adspecies of high OCM selectivity.

In any metal oxide catalyst with stable cationic valency, electrons for the reduction of adsorbates can only come from the O^{2-} ions. The reduction of each $\underline{O}_2$ adspecies to $\underline{O}_2^-$ or $\underline{O}_2^{2-}$ adspecies is accompanied by the formation of, respectively, one or two $\underline{O}^-$ in the oxide lattice. Though some of $\underline{O}^-$ ions might tug away in the bulk [104], still there would be quite a large number of $\underline{O}^-$ in the surface lattice in the absence of some way to tie them up. The $\underline{O}^-$ ions are known to be highly reactive, capable of attacking C_2H_4 even at a very low temperature [104]. In the absence of some way to tie the $\underline{O}^-$ up, how could high C_2^+ selectivity at moderate level of methane conversion be actually obtained with many of the OCM catalysts with stable cationic valency? But the most interesting puzzle is the absence of Raman signal of $\underline{O}_2^-$ when the rare-earth-oxide-based catalyst is in contact with pure O_2 at 0.1 MPa, in contrast with the presence of clearly observable Raman signal of $\underline{O}_2^-$ when the catalyst is in contact with CH_4–O_2 in the feed with P_{O_2} only about 0.02–0.002 MPa at the reactor entry.

In an attempt to solve these puzzles, it has been suggested by Tsai et al. [83] that there might be certain elusive precursor of $\underline{O}_2^-$, which might be present in very low concentration in OCM, but much more reactive than $\underline{O}_2^-$ towards CH_4, and that it might react with CH_4 with the formation of $\underline{O}_2^-$ besides hydrocarbon products. It has been speculated by these authors [83] that O_3^{2-} might be formed by incorporation of $\underline{O}_2$ adspecies with a neighbouring $\underline{O}^{2-}$ ion at about 2.7–2.9 Å nucleus-to-centre distance from the anionic vacancy occupied by $\underline{O}_2^-$. The process of this incorporation may be envisaged as follows. An O_2 molecule adsorbs reversibly at the anion-vacant site, the diatomic adspecies $\underline{O}_2$ abstracts an electron from a neighbouring O^{2-} ion, resulting in the formation of two radicals ($\underline{O}_2^-$ and $\underline{O}^-$) at neighbouring sites. $\underline{O}_2^-$ is known to be both Raman and IR active [98], so it is not likely to be a flat-lying adspecies. In the absence of steric hindrance by neighbouring adsorbate, the two radicals may then unite to form the triatomic, angular anionic adspecies, $\underline{O}_3^{2-}$, thus tying up the damaging $\underline{O}^-$ species. This process is shown as the dotted rectangular box in Scheme 4.

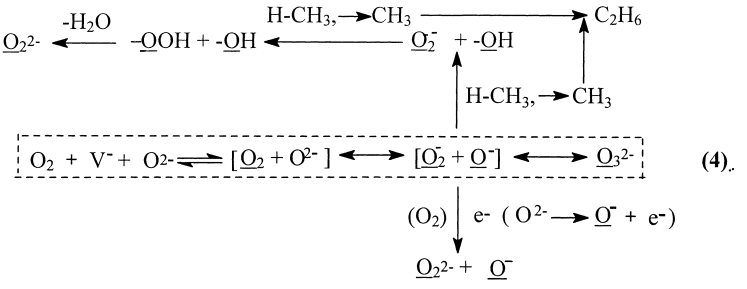

Scheme 4.

The internuclear distance between the two terminal-O of the angular $\underline{O}_3^{2-}$ is estimated to be about 2.52 Å, with the bond angle taken to be ca.116.8°, as that of O_3 [112] and the O–O single-bond length about 1.48 Å [19]. On the surface of a host rare-earth oxide (e.g., on the non-polar (1 1 0) surface of La^{3+}-doped or Sr^{2+}-doped ThO_2 (DFS), or the non-polar (1 1 0) minor surface of Ca^{2+}-doped, hexagonal La_2O_3) the closest anionic–anionic internuclear distance of two O^{2-} ions, or an O^{2-} and an anionic vacancy is about 2.8 Å. So, in the absence of steric hindrance imposed by neighbouring adsorbate, the angular $\underline{O}_3^{2-}$ should be able to stretch the distance of its two terminal-O by ca. 0.3 Å, and adapt itself (with approximate C_{2v} symmetry) to the twin-sites of the surface lattice (Fig. 7).

The reactivity of this active precursor species in OCM may be envisaged as follows. In H-abstraction from CH_4, this active precursor might react like a bi-radical, $[\underline{O}_2^-, \underline{O}^-]$ to form CH_3, –$\underline{O}$H, and $\underline{O}_2^-$ since H-abstraction activity of $\underline{O}^-$ is known to be much higher than that of $\underline{O}_2^-$. On the other hand, in a flow of O_2 with no hydrocarbons, O_3^{2-} might capture an electron from the oxide lattice and be reduced to form O_2^{2-} plus $\underline{O}^-$, rather than $\underline{O}_2^-$ plus $\underline{O}_2^-$, since the binuclear $\underline{O}_2^-$ is more electrophilic than $\underline{O}^-$. These two different pathways are shown in the central part of Scheme 4 above and below the dotted frame. (In the dotted frame of Scheme 4, resonance hybrid structures are connected by double-headed arrows, and anionic vacancy denoted by V^-.) The $\underline{O}^-$ is likely to react with CH_4 considerably more slowly than its active precursor species $\underline{O}_3^{2-}$, of which the reactivity might be between that of $\underline{O}_2^{2-}$ and $\underline{O}_2^-$ in H-abstraction from CH_4. So a dynamic concentration of $\underline{O}_2^-$ may be built up to Raman spectroscopically detectable level, though it is likely that some of the O_2^- ions may be further reduced to $\underline{O}_2^{2-}$. Collision of the newly produced CH_3 with $\underline{O}H^-$ will be harmless, resulting in no further H-abstraction. Collision of CH_3 with $\underline{O}_2^-$ will also be relatively harmless since H-abstraction from CH_3 by $\underline{O}_2^-$ is weak (as can be inferred from the low BE of 87 kcal/mol for H–OOH, and the relatively high BE of H–CH_2, 110 kcal/mol, ca. 5 kcal/mol higher than that of H–CH_3) [19]. Moreover, at moderate level of methane conversion, there are more CH_4 molecules than CH_3 radicals around each site. So the chance of H-abstraction from CH_4 by $\underline{O}_2^-$ is much greater than that from CH_3. Thus at OCM temperature when $\underline{O}_2^-$ is sufficiently active, there is a good chance for the production and coupling of two CH_3 radicals formed successively from two CH_4 molecules via H-abstraction by the resonance hybrid of $\underline{O}_3^{2-}$, concomitant with the successive formation of $\underline{O}H^-$ and $^-\underline{O}OH$ followed by dehydration to give $\underline{O}_2^{2-}$. The sequence of reactions may take place so fast that most of the first CH_3 and the –OH formed cannot have time to diffuse or migrate away. The sequence of reactions is shown at the right and left corners above the dotted frame of Scheme 4. Thus the attainable high C_2^+ selectivity can be explained.

The angular $\underline{O}_3^{2-}$ species may dissociate from either one of the two O–O single bonds for O_2 to desorb reversibly from either side; thus the rapid oxygen isotope exchange with labelled O_2 and a doped REO_2 or Ln_2O_3 can be explained.

From the known O–O stretching frequencies of O_2 (ν_{O-O}=1550 cm^{-1}), Ba^{2+}-bound $\underline{O}_2^-$ and $\underline{O}_2^{2-}$ (cf. Fig. 4A, ν_{O-O}=1122 and 840 cm^{-1}, respectively), and O_3 (ν_1=1136 cm^{-1}), $\underline{O}_3^-$ (ν_1=1016 cm^{-1} [113]), the Raman-active ν_1 of $\underline{O}_3^{2-}$ may be roughly estimated to be around 900–950 cm^{-1}, depending on the micro-environment. A check of the frequency

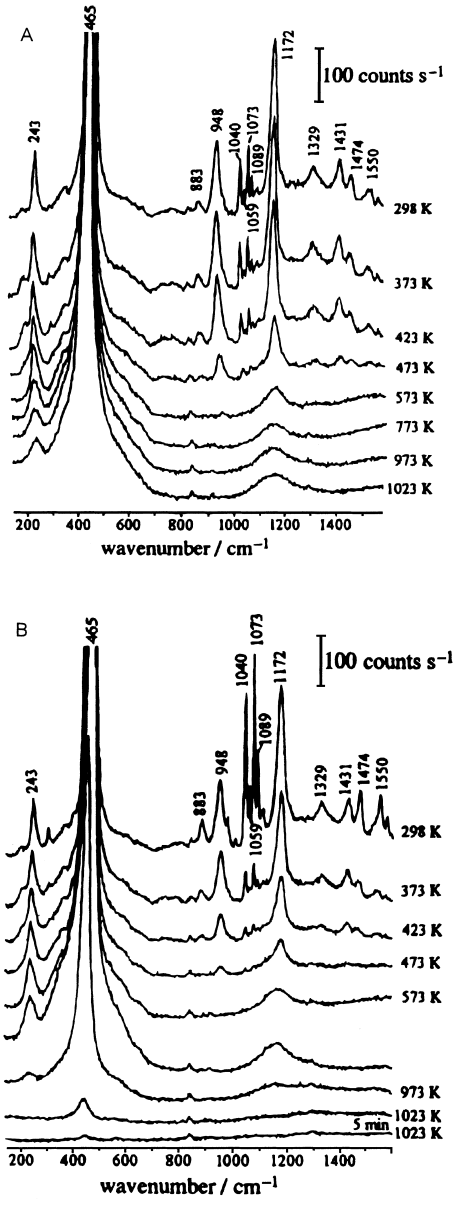

Fig. 7. Reproduced from [98]: Microprobe Raman spectra of O_2-pretreated BaF_2/CeO_2 (Ba:Ce=4:1) catalyst at the indicated temperature in A: Helium, and B: C_2H_6 atmosphere.

range and H-abstraction reactivity of $\underline{O}_3^{2-}$ by quantum-chemical calculations with embedded cluster model analogous to that used by Borce and Patterson [114] is in progress.

The species with Raman signal at 940 cm^{-1} (mw) in the in situ Raman spectrum (Fig. 5C) of Th–La–O_x/$BaCO_3$ catalyst in flowing CH_4–O_2 (4:1) at 773 K (along with the two $\underline{O}_2^-$ Raman signals at 1120 (mw) and 1148 cm^{-1} (mw)) observed by Zhang et al. [85] may be the elusive $\underline{O}_3^{2-}$ species they have been looking for as the active precursor of $\underline{O}_2^-$ and $\underline{O}_2^{2-}$.

In some systems, O_2 may adsorb at an F-centre to form $\underline{O}_2^-$. There may also be some sites where $\underline{O}_3^{2-}$ may not be formed due to steric hindrance, or lack of neighbouring O^{2-} at suitable distance, then $\underline{O}_2^-$ may be formed from $\underline{O}_2$ by electron transfer from the oxide lattice.

Biphasic REO–AEO OCM catalysts with DFS have been prepared by Liu et al. [82,87] by co-precipitation method. The Th–La–Ca–Ba–O/(Ba,Ca)CO_3 catalyst thus prepared showed very high stability (no change in performance after 1000 h micro-reactor evaluation at 1053 K plus intensified sintering test by heating at 1273 K for 1 h), high CH_4 conversion (ca. 33% at 6×10^4 h^{-1} GHSV), C_2 selectivity (~62%; 65.7% in terms of C_2^+) and C_2 yield (~20.5%, ~3% higher than that of $La_2O_3/BaCO_3$ catalysts under the same conditions). Thus $\chi+S\approx99\%$. Further improvement in micro-reactor performance via composition optimisation may be expected. But the catalyst was found to deactivate rapidly due to hot spots overheating in an adiabatic stationary-bed reactor with 50 ml sample. So there are also engineering design problems to be solved.

5.2. *Systematic studies of novel REO(F)–AEO(F) catalysts for OCM, ODE, and ODP*

Since there is a review by Wan et al. [90] of this work, here only a brief account is given.

The study of fluoride doping of REO–AEO-based catalyst systems was started by one of our research groups in 1992, drawing inspiration from the work of Lunsford et al. [75,78] showing the marked enhancement of C_2H_4 selectivity by doping some OCM and ODE catalysts with chlorides. Further elaboration of the idea of fluoride-doping was guided by structure–function relationship consideration and experimental development. The anionic radii of F^- (1.33 Å) and O^{2-} (1.32 Å) are almost equal, but the ionisation potential of F^- is much higher than that of O^{2-}. The crystal habits of most of the alkaline-earth fluorides (MF_2), lanthanide oxides (LnO_2), sesquioxides (Ln_2O_3), and oxyfluorides (LnOF) are quite similar

[19,115–118] being the cubic fluorite structure and defective fluorite structure, or slightly distorted fluorite structures with tetragonal, or rhombohedral settings. So wide ranges of mutual solubility of the MF_2 and the REO_2, Ln_2O_3, or LnOF may be expected, with wide ranges of anionic vacancy concentrations and anionic mobility, and wide ranges of modification of work functions, surface basicity and resistance to CO_2 inhibition. The fluoride ions may also serve to disperse the various active-oxygen species to decrease deep oxidation of the hydrocarbons.

The results from the studies of fluoride-containing catalysts are summarised below.

With lanthanide ions of stable valency (e.g., La^{3+}, Nd^{3+}, Sm^{3+}, Gd^{3+}, and Y^{3+}), the 20–50 mol% SrF_2–Ln_2O_3 catalyst systems showed higher C_2-selectivity (57.3–54.6%), and on the average slightly higher ethylene selectivity than that of the corresponding REO–AEO catalysts. However, the possible effect of "hot spot" temperature on the precision of the temperature measurements must be taken into consideration. Results of catalyst evaluation of these SrF_2–Ln_2O_3 catalysts with stable cationic valency show that the higher the anionic conductivity of the Ln_2O_3 the slightly higher the C_2 selectivity. This is also the order of increasing Ln^{3+} ionic sizes, with the exception of Y_2O_3 with comparatively smaller size of Y^{3+}, but somewhat higher oxide-ion conductivity and higher C_2 selectivity [93,94]. With lanthanide ions of variable valency (e.g., $Ce^{3+/4+}$), replacement of the AEO in the REO–AEO composite-oxides by BaF_2 (or SrF_2) has the marvellous effect of changing the deep-oxidation catalysts (e.g., CeO_2–AEO), into good OCM catalysts (e.g., CeO_2/BaF_2, 54.6% C_2 selectivity and 17.6% C_2 yield at 1073 K) and excellent ODE catalysts [90–95]. As shown by in situ microprobe Raman spectra of O_2-pretreated CeO_2–BaF_2 [90–93,98], the $\underline{O}_2^-$ with Raman band at 1172 cm^{-1} (s–m–w, under helium atmosphere at 298–373–973 K) and lattice O^{2-} (probably only those associated with Ce^{4+}) with lattice-vibration band at 465 cm^{-1} (very strong, even at 1023 K under helium atmosphere) were observed, along with a medium-to-weak band at 243 cm^{-1}. These have been assigned, respectively, to F_{2g} mode and TO (transverse optical) mode of lattice vibrations of slightly distorted CeO_2 with DFS. So they are both related to Ce^{4+}–O^{2-}. Each of these two bands appeared to be affected separately to different extent by CH_4, C_2H_6, and C_2H_4 in the order of increasing rates, and disappeared in the order of markedly decreasing times at 1023 K. Thus $\underline{O}_2^-$ and the lattice O^{2-} backed up by Ce^{4+} must be regarded here as significant active-oxygen species [90,98]. There was an unidentified species with Raman band at 948 cm^{-1} (ms at 298 K, m at 373 K, wm at 423 K, and w at 473 K, w at 573 K); the signal fell below detection limit above 573 K under He, or above 473 K under C_2H_6 atmosphere [90,98]. This may be compared with the species with Raman signal at 940 cm^{-1} on Th–La–O_x/$BaCO_3$ catalyst (Fig. 5C(b)) in flowing CH_4–O_2 (4:1) at 773 K observed by Zhang et al. [85] (Fig. 8). There was a Raman band at 1550 cm^{-1} (w at 298 K, vw at 373 K), ascribable to $\underline{O}_2$ adspecies. There were also Raman bands at 1040 (m), 1073 (m), 1089 (w), 1329 (wm), 1431 (w), and 1474 cm^{-1} (w), all of these signals fell below detection limit above 473 K under either He or C_2H_6 atmosphere. Compared with the known Raman spectra of O_2-pretreated $La_2O_3/BaCO_3$ catalysts taken in argon at room temperature, these may be assigned to three carbonate species at different micro-environments (although the possibility of over-lapping with some other $\underline{O}_2^-$ species and some other $\underline{O}_2$ species cannot be ruled out). These surface carbonate species might have come from combustion of carbonaceous contaminants during the O_2-pretreatment of the catalyst, and they were easily removed by heating the catalyst sample in helium to 473 K due to the much lower basicity of 20 mol% BaF_2/CeO_2 than that of

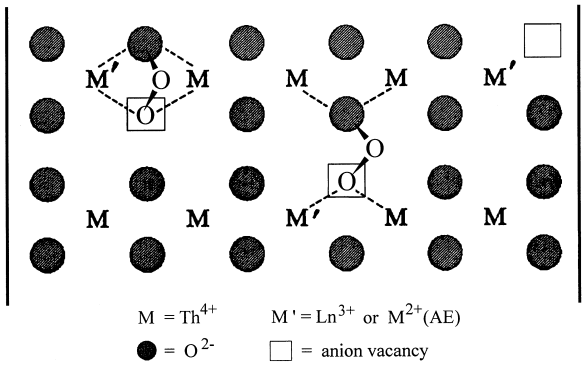

Fig. 8. A model of probable structure of $\underline{O}_3^{2-}$ ($\sim C_{2v}$, internuclear distance O(1)–O(3) of angular $\underline{O}_3^{2-} \geq 2.5$ Å). on Ln_2O_3–ThO_2 (uniphasic, DFS, closest O–O≈2.7–2.8 Å (1 1 0) surface.

$La_2O_3/BaCO_3$. It is interesting to note that the O_2-pretreated catalyst sample under CH_4 atmosphere at 573–773–973–1023 K gave microprobe Raman band at 1165 cm^{-1} (s–s–s–ms, the signal fell below detection limit after heating the system at 1023 K for 10 min), and another band at ca. 840 cm^{-1} (w–w–w–w, persisting after heating the system at 1023 K for 10 min and becoming very weak (vw) after heating the system for 40 min); no other bands being observed in the range 800–1400 cm^{-1}. The first Raman band may be ascribed to $\underline{O_2^-}$ and the second to $\underline{O_2^{2-}}$, as a downstream adspecies in further reduction of $\underline{O_2^-}$. Note also that with O_2-pretreated catalyst sample in a flow of CH_4–O_2 (3.4:1) at 923, 973, and 1023 K, only a strong Raman band of $\underline{O_2^-}$ at 1153 cm^{-1} was observed in the wave number range 780–1500 cm^{-1}, indicating that this superoxide adspecies was steadily produced at these temperatures, to practically saturated, dynamic concentration, from a much more reactive precursor oxygen-species. The downstream peroxide adspecies at these temperature was too reactive to give detectable Raman signal, as in the case of OCM reaction over Ba^{2+}/MgO [106].

Conceivably, due to the higher work function of a fluoride-containing REO–AEO-based catalyst than that of the corresponding REO–AEO catalyst, $\underline{O_2^-}$ adspecies on the fluoride-containing catalyst may not be so easily reduced further to form the downstream adspecies, $\underline{O_2^{2-}}$ and $2\underline{O^-}$, thus making it possible to detect the $\underline{O_2^-}$ on O_2-pretreated sample by in situ FTIR and Raman spectroscopic techniques, and to study its reaction with methane, or other reactants. $\underline{O_2^-}$ adspecies on O_2-pretreated SrF_2/La_2O_3 with Raman bands at 1113 cm^{-1} (923 K) have been found to react with CH_4 with the formation of C_2H_4, CO_2, and surface carbonate; and likewise $\underline{O_2^-}$ adspecies with Raman band at 1114 cm^{-1} on SrF_2/Nd_2O_3 at 973 K [90–93]. Thus for the first time, direct evidence for $\underline{O_2^-}$ being a principal OCM-active oxygen-adspecies was obtained. It has also been demonstrated that there is no simple dependency of catalyst activity and selectivity for OCM and ODE on catalyst surface basicity–acidity, and that p-type conductivity is not always required for good OCM performance [90–93].

Based upon the principle of structure-directed constituent selection [95–97], a series of BaF_2-doped, tetragonal LaOF catalysts showing excellent performance for both OCM and ODE were prepared. With a 10 mol% BaF_2/LaOF catalyst for OCM, under the conditions of 1043 K, $CH_4/O_2=6$, and GHSV=15 000 h^{-1}, methane conversion (χ) of 19.5% and C_2 selectivity (S) of 81.2% were obtained [90,93], $\chi+S$ exceeding 100%. With a 30 mol% BaF_2/LaOF catalyst for ODE, under the conditions of 913 K, $C_2H_6/O_2=2$, GHSV=11 600 h^{-1}, C_2H_6 conversion of 80.8% and C_2H_4 selectivity of 70.8% were obtained [96,97]. Although, the graduate, hydrolytic loss of fluoride (HF) at high reaction temperature is still quite a problem for these fluoride-containing REO–AEO-based catalyst systems, they may find application in some other oxidative–coupling, or oxidative–dehydrogenation reactions that can take place at lower temperatures. More importantly, the systematic studies of these halide-containing REO–AEO-based catalyst systems have already furnished important information for clarifying some controversial issues, establishing some fundamental principles for host and dopant constituents selection, and opening the way for further research. For example, by proper design of experiments, it may be possible to reveal the mechanistic mystery of the remarkable promotion of ethylene selectivity by halide-doping of the OCM and ODE catalysts.

6. Concluding remarks

Most of the research work reviewed in this paper was done in the last 10 years or so (picking up speed with the development of postgraduate research programme and reconstruction of the SKLPCSS), with the main objective of co-ordinating with the expected development of power industry in China based on coal, as well as on natural gas, by the integrated gasification and combined cycles (IGCCs) technology, for co-production of liquid fuels and basic organic chemicals with the generation of electric power. Over the past 40 years, 19 Chinese patents were obtained, most of them in the last few years. There has been more recent research work done by our team in other areas related to applied catalysis; this is not covered in this review, though there have been some very interesting results, such as new catalytic materials [118] and new catalytic processes [119], exhaust pollution control catalysts for methanol-fuelled automobiles [120], high enantio-selective catalysts for asymmetric

transfer-hydrogenation of carbonyl functions [121, 122], supported liquid-phase catalysts for olefin hydroformylation [123], K_2O-promoted iron oxides-based catalysts for ethyl-benzene dehydrogenation [124,125] (which has been commercialised by the chemical plant at Xiamen University by supplying to about a dozen small styrene plants in China for more than 10 years), structural basis for catalysts preparation by the citrate-complex method [126,127], and computer-aided catalyst design [128]. It may be expected that these recent achievements in catalysis will be reviewed in the near future by the young, principal investigators themselves.

Acknowledgements

The support of this work by the State Science and Technology Commission and National Natural Science Foundation of China is gratefully acknowledged.

References

[1] Yu.A. Gorin, Chem. Ind. (Russ.) (1959) 1944.
[2] Yu.A. Gorin et al., Chem. Ind. (Russ.) (1964) 265.
[3] Xiamen Acetic Acid Factory, Xiamen Synth. Rubber Processing Factory, Chemistry Department, Xiamen University, Acta Chim. Sinica (Chinese) 3 (2) (1975) 114.
[4] Catal. Div., Chemistry Department, Xiamen University, Scientia Sinica (Chinese) (1973) 373.
[5] J.L. Zeng et al., CN Patent No. 85102996.5.
[6] W.Z. Weng et al., Chem. J. Chinese Univ. B (4) (1990) 346.
[7] K. Tamaru, Catal. Rev. 4 (1970) 161.
[8] K.R. Tsai, in: W.E. Newton, W.H. Orme-Johnson (Eds.), Nitrogen Fixation, vol. I, University Park Press, Baltimore, USA, 1980 p. 373; Scientia Sinica (Engl. Ed.) (1976) 460.
[9] K.R. Tsai, H.L. Wan, in: M. Tsutsui, Y. Ishi, Y.-Z. Huang (Eds.), Fundamental Research in Organometallic Chemistry, University Park Press, Baltimore, USA, 1982, p. 1.
[10] K.R. Tsai, H.-B. Zhang, G.D. Lin, Adv. Sci. China, Chem. 2 (1987) 125.
[11] K.H. Huang, in: A.T. Seiyama, D.K. Tanabe (Eds), Proceedings of the Seventh International Congress on Catalysis, New Horizons in Catalysis, Studies in Surface Science and Catalysis, vol. 7, Kodansha, Tokyo, 1981, p. 554.
[12] D.W. Liao, H.B. Zhang, Z.Q. Wang, K.R. Tsai, Scientia Sinica, Ser. B (Engl. Ed.) (1987) 246.
[13] H.B. Zhang, K.R. Tsai, Catal. Lett. 3 (1989) 129.
[14] K.R. Tsai, H.L. Wan, J. Cluster Sci. 6 (1895) 485.
[15] H.L. Wan, J.W. Huang, F.Z. Zhang, Y. Wu, L.S. Xu, J.L. Li, K.R. Tsai, in: C. Elmerich et al. (Eds.), Biological Nitrogen Fixation for the 21st Century, Kluwer Academic Publishers, Dordrecht, 1998, p. 78.
[16] K. Klier, Adv. Catal. 31 (1982) 243.
[17] G.A. Vedage, R. Pitchai, R.G. Herman, K. Klier, in: Proceedings of the Eighth International Congress on Catalysis, Berlin, vol. 2, 1984, p. 47.
[18] J. Halpern, Acc. Chem. Res. 15 (1982) 238.
[19] CRC Handbook of Chemistry and Physics, 66th ed., 1985.
[20] H. Chen, S. Wang, Y. Liao, J. Cai, H. Zhang, K. Tsai, in: Proceedings of the Third China–Japan–USA Symposium on Catalysis, Xiamen, 1987, p. 97.
[21] H. Chen, S. Wang, Y. Liao, J. Cai, H. Zhang, K. Tsai, in: Proceedings of the Ninth International Congress on Catalysis, Calgary, 1988, p. 537.
[22] M.A. Bennett, J. Mol. Catal. 41 (1987) 1.
[23] J.F. Edwards, G.L. Schrader, J. Phys. Chem. 89 (1985) 782.
[24] J.C. Lavalley, J. Saussey, T. Rais, A. Chakor-Alami, J.P. Hindermann, A. Kiennemann, J. Mol. Catal. 26 (1984) 159.
[25] H. Idress, J.P. Hindermann, A. Kiennemann et al., J. Mol. Catal. 42 (1987) 205 and relevant references cited.
[26] M.-Y. He, J.G. Ekerdt, J. Catal. 87 (1984) 237.
[27] M.-Y. He, J.G. Ekerdt, J. Catal. 87 (1984) 381.
[28] R. Burch, R.J. Chappell, S.E. Golunski, J. Chem. Soc., Faraday Trans. I 85 (1989) 4569.
[29] D. Duprez, Z. Ferhat-Hamida, M.M. Bettanar, J. Catal. 124 (1990) 1.
[30] J. Cai, Y. Liao, H. Chen, K. Tsai, in: Proceedings of the 10th International Congress on Catalysis, Budapest, 1992, p. 2769.
[31] G.C. Chinchen, M.S. Spenser, K.C. Waugh, D.A. Whan, Faraday Symp. Chem. Soc. 21 (1986) 21 (Paper 18).
[32] G.C. Chinchen, P.J. Denny, J.R. Jennings, M.S. Spenser, K.C. Waugh, Appl. Catal. 36 (1988) 1–65.
[33] K.C. Waugh, Catal. Today 18 (1993) 147.
[34] J.C.J. Bart, R.P.A. Sneeden, Catal. Today 2 (1987) 1.
[35] G. Ghiotti, F. Boccuzzi, Catal. Rev.-Sci. Eng. 29 (1987) 151.
[36] A. Cybulski, Catal. Rev.-Sci. Eng. 36 (1994) 557.
[37] Y.Q. Yang, H.B. Zhang, G.D. Lin, H.Z. Chen, Y.Z. Yuan, K.R. Tsai, J. Xiamen Univ. 33 (1994) 477.
[38] Y.F. Shen, L.F. Cai, J.T. Li, S.J. Wang, K.H. Huang, Catal. Today 6 (1989) 47.
[39] Y.F. Shen, S.J. Wang, K.H. Huang, Appl. Catal. 57 (1990) 55.
[40] Y.F. Shen et al., Appl. Catal. 59 (1990) 61.
[41] T.P. Wilson, P.H. Kasai, P.C. Ellgen, J. Catal. 69 (1981) 193.
[42] M. Ichikawa, T. Fukushima, K. Sikakura, in: Proceedings of the Eighth International Congress on Catalysis, Berlin, vol. 2, 1984, p. 69.
[43] S.J. Tauster et al., J. Am. Chem. Soc. 100 (1978) 170.
[44] W.M.H. Sachtler, in: Proceedings of the Eighth International Congress on Catalysis, Berlin, vol. 1, 1984, p. 151.
[45] W.M.H. Sachtler, M. Ichikawa, J. Phys. Chem. 90 (1986) 4752.
[46] S. Orita, S. Naito, K. Tamaru, J. Catal. 90 (1984) 183.
[47] J.S. Rieck, A.T. Bell, J. Catal. 113 (1985) 341.

[48] A.T. Bell, J. Mol. Catal. 100 (1995) 1–11.
[49] A. Takeuchi, J.R. Katzer, J. Phys. Chem. 86 (1982) 2438.
[50] A. Deluzarche, J.P. Hindermann, R. Kieffer et al., J. Phys. Chem. 88 (1984) 4493.
[51] T. Mori, H. Masuda, H. Imal, J. Phys. Chem. 86 (1972) 2753.
[52] M.A. Logan, G.A. Somorjai, J. Catal. 85 (1985) 317.
[53] G.S. Gu, J.P. Liu, J.K. Fu, K.R. Tsai, Acta Phys. Chim. Sinica 1 (1985) 177.
[54] J.P. Liu, H.Y. Wang, J.K. Fu, Y.G. Li, K.R. Tsai, in: Proceedings of the Ninth International Congress on Catalysis, Calgary, 1988, p. 735.
[55] J.P. Liu, H.Y. Wang, J.K. Fu, Y.G. Li, K.R. Tsai, Proceedings of the Third China–Japan–USA Symposium on Catalysis, Xiamen, 1987, p. 99.
[56] P.T. Wolczanski, J.E. Bercaw, Acc. Chem. Res. 13 (1980) 121.
[57] P.H. McBreen, W. Erley, H. Ibach, Surf. Sci. 148 (1984) 292.
[58] A. Deluzarche, J.P. Hindermann, A. Kiennemann, J. Mol. Catal. 31 (1985) 225.
[59] H.Y. Wang, J.P. Liu, J.K. Fu, H.B. Zhang, K.R. Tsai, Catal. Lett. 12 (1992) 87.
[60] H.Y. Wang, J.P. Liu, J.K. Fu, H.L. Wan, K.R. Tsai, Res. Chem. Interm. 17 (1992) 233.
[61] Y.H. Du, D.A. Chen, K.R. Tsai, Appl. Catal. 35 (1987) 77.
[62] Y.M. Hu, H.Y. Wang, J. Mol. Catal. (China) 7 (1993) 119.
[63] J.P. Hindermann, G.J. Hutchings, A. Kienemann, Catal. Rev. 39 (1993) 1–127.
[64] H.Y. Wang, J.P. Liu, K.R. Tsai, in: K.R. Tsai, S.Y. Peng et al. (Eds.), Catalysis in C_1 Chemistry, Chem. Ind. Press, Beijing, 1995, pp. 167–186.
[65] J.K. Fu, J.L. Xu, J.P. Liu, H.Y. Wang, K.R. Tsai, J. Xiamen Univ. (Nat. Sci.) 32 (1993) 604.
[66] H.Y. Wang, J.P. Liu, K.R. Tsai, J. Mol. Catal. (China) 5 (1991) 16.
[67] M. Ichikawa, in: Y. Iwasawa (Ed.), Tailored Metal Catalysis, Reidel, Dordrecht, 1986, p. 183.
[68] H.Y. Wang, K.R. Tsai, Hua Xue Tong Bao 9 (1997) 1.
[69] S.S.C. Chuang, S.I. Pien, J. Catal. 138 (1992) 536.
[70] S.S.C. Chuang et al., Appl. Catal. A 151 (1997) 334.
[71] H.Y. Wang, J.P. Liu, J.K. Fu, K.R. Tsai, Acta Phys. Chim. Sinica 7 (1991) 681.
[72] H.Y. Wang, J.P. Liu, K.R. Tsai, J. Mol. Catal. (China) 8 (1994) 472–486.
[73] G.E. Keller, M.M. Bhasin, J. Catal. 73 (1982) 9.
[74] W. Hinsen, M. Baerns, Chem. Ztg. 107 (1983) 229.
[75] J.H. Lunsford, Angew. Chem., Int. Ed. Engl. 34 (1995) 970–980.
[76] G.J. Hutchings, M.S. Scurrell, in: E.E. Wolf (Ed.), Methane Conversion by Oxidative Processes, Van Nostrand Reinhold, New York, 1992, pp. 201–258.
[77] M. Baerns, J.R.H. Ross, in: J.M. Thomas, K.I. Zamaraev (Eds.), IUPAC Monograph Perspective in Catalysis, 1990, pp. 315–334.
[78] J.H. Lunsford, Catal. Today 6 (1990) 235.
[79] Z. Kalenik, E. Wolf, Catal. Today 13 (1992) 255–264.
[80] Z.L. Zhang, C.T. Au, K.R. Tsai, Appl. Catal. 62 (1990) L29.
[81] Y.D. Liu, G.D. Lin, H.B. Zhang, J.X. Cai, H.L. Wan, K.R. Tsai, in: Preprints Fuel. Chem. Div., ACS National Meeting, San Francisco, vol. 37, no. 1, 1992, p. 356.
[82] Y.D. Liu, H.B. Zhang, G.D. Lin, K.R. Tsai, in: K.R. Tsai, S.Y. Peng et al. (Eds.), Catalysis in C_1 Chemistry, Chem. Ind. Press, Beijing, 1995, p. 46.
[83] Y.D. Liu, G.D. Lin, H.B. Zhang, K.R. Tsai, in: H.E. Curry-Hyde, R.F. Howe (Eds.), Natural Gas Conversion II, Elsevier, Amsterdam, 1994, p. 131.
[84] Y.D. Liu, H.B. Zhang, G.D. Lin, Y.Y. Liao, K.R. Tsai, J. Chem. Soc., Chem. Commun. (1994) 1871.
[85] H.B. Zhang, Y.D. Liu, G.D. Liu, Y.Y. Liao, K.R. Tsai, 207th ACS National Meeting, 1994, Abstracts of Papers (2), PHYS 0277, submitted for publication.
[86] J.X. Cai, A.M. Huang, Y.Y. Liao, H.L. Wan, in: N.T. Yu, X.Y. Li (Eds.), Proceedings of the Fourth International Conference on Raman, Wiley, New York, 1994, p. 526.
[87] K.R. Tsai, H.L. Wan, H.B. Zhang, G.D. Lin, invited paper, Sect. 5, 34th IUPAC Congress, Beijing, 1993, in: Book of Abstracts, p. 671, submitted for publication.
[88] J.L. Dubois, C.J. Cameron, Appl. Catal. 67 (1990) 49.
[89] A.G. Anshits, E.N. Voskesenkaya, L.I. Kurteeva, Catal. Lett. 6 (1990) 49.
[90] H.L. Wan, W.Z. Weng, Y. Iwasawa, Hyomen (Surface) 36 (1998) 53.
[91] X.P. Zhou, S.Q. Zhou, W.D. Zhang, Z.S. Chao, W.Z. Weng, R.Q. Long, D.L. Tang, H.Y. Wang, J.X. Cai, H.L. Wan, K.R. Tsai, 207th ACS National Meeting, Preprints Div. Petro. Chem. Inc. 39 (1994) 222.
[92] M.M. Bhasin, D.W. Slocum (Eds.), Methane and Alkane Conversion Chemistry, Plenum, New York, 1995, p. 19.
[93] R.Q. Long, S.Q. Zhou, Y.P. Huang, W.Z. Weng, H.L. Wan, K.R. Tsai, Appl. Catal. A 133 (1995) 269.
[94] R.Q. Long, Y.P. Huang, W.Z. Weng, H.L. Wan, K.R. Tsai, Catal. Today 30 (1996) 59.
[95] Z.S. Chao, X.P. Zhou, H.L. Wan, K.R. Tsai, Appl. Catal. A 130 (1995) 127.
[96] X.P. Zhou, Z.S. Chao, J.Z. Luo, H.L. Wan, K.R. Tsai, Appl. Catal. A 133 (1995) 263.
[97] H.L. Wan, Z.S. Chao, W.Z. Weng, X.P. Zhou, J.X. Cai, K.R. Tsai, Catal. Today 30 (1996) 67.
[98] R.Q. Long, H.L. Wan, J. Chem. Soc., Faraday Trans. 93 (1997) 355.
[99] K. Nakamoto, Infrared and Raman Spectra of Inorganic and Coordination Compounds, 4th ed., Wiley, New York, 1986.
[100] Y. Osada, S. Kolke, T. Fukushima, S. Ogasawara, Appl. Catal. 59 (1990) 59.
[101] T.-L. Yang, L.-B. Feng, S.K. Shen, J. Catal. 145 (1994) 384.
[102] C. Louis, T.L. Chang, M. Kermarec, T.L. Van, J.M. Tatibouet, M. Che, Catal. Today 13 (1992) 283.
[103] Y.Y. Liao, P.H. Hong, J.X. Cai, in: N.T. You, X. Y. Li (Eds.), Proceedings of the Fourth International Conference on Raman Spectroscopy, Wiley, New York, 1994, p. 1086.
[104] M. Che, G.C. Bond (Eds.), Adsorption and Catalysis on Oxide Surfaces, Studies in Surface Science and Catalysis, vol. 21, Chapters 1 and 2, Elsevier, Amsterdam, 1985, pp. 1 and 11.

[105] D. Mestl, H. Knoginger, J.H. Lunsford, Ber. Bunsenges. Phys. Chem. 97 (1993) 319.
[106] J.H. Lunsford, X. Yang, K. Haller, J. Laane, G. Mestl, H. Knozinger, J. Phys. Chem. 97 (1993) 13810.
[107] L. Dubois, M. Bisiaux, M. Mimoun, C.J. Cameron, Chem. Lett. (1990) 967.
[108] L. Dubois, M. Bisiaux, M. Mimoun, C.J. Cameron, Chem. Lett. (1991) 1089.
[109] K. Otsuka, A.A. Said, K. Jimmo, Komatsu, Chem. Lett. (1987) 77.
[110] Otsuka et al., Chem. Lett. (1986) 967.
[111] A. Bielanski, J. Haber, Catal. Rev.-Sci. Eng. 19 (1979) 1.
[112] N.W. Greenwood, A. Earushaw, Chemistry of the Elements, Pergamon Press, Oxford, 1984, pp. 707–711.
[113] L. Andrews, P.C. Spiker Jr., , J. Chem. Phys. 59 (1973) 863.
[114] K.J. Borve, Pettersson, J. Phys. Chem. 95 (1991) 3214.
[115] A.F. Wells, Structural Inorganic Chemistry, 5th ed., Oxford University Press, New York, 1984, pp. 545–546.
[116] W.H. Zachariasen, Acta Cryst. 4 (1951) 231.
[117] D.B. Shinn, H.A. Eick, Inorg. Chem. 8 (1969) 232–235.
[118] P. Chen, H.B. Zhang, G.D. Lin, Q. Hong, K.R. Tsai, CARBON 35(10)(11) (1997) 1495.
[119] H.B. Zhang, H.Y. Li, G.D. Lin, K.R. Tsai, in: J.W. Hightower, W.N. Delgass, E. Iglesia, A.T. Bell (Eds.), Proceedings of the 11th ICC, Stud. Surf. Sci. Catal. 101 (1996) 1369.
[120] L.F. Yang, D.H. Chen, J.X. Cai, H.L. Wan, in: Proceedings of the APCAT'97, South Korea, 1997, p. 183.
[121] J.X. Gao, P.P. Xu, P.Q. Huang, H.L. Wan, K.R. Tsai, J. Mol. Catal. (China) 11 (1997) 413.
[122] J.X. Gao, T. Ikariya, R. Noyori, Organometallics 15 (1996) 1087.
[123] Y.Z. Yuan, J.L. Xu, H.B. Zhang, K.R. Tsai, Catal. Lett. 29 (1994) 387.
[124] H.Z. Chen, D.Y. He, Z.L. Xiao, K.R. Tsai, Chem. J. Chinese Univ. 6 (1985) 433.
[125] J.P. Chen, D.Y. He, S.J. CAO, Chem. J. Chinese Univ. 7 (1986) 1020.
[126] Z.H. Zhou, Y.J. Lin, H.B. Zhang, G.D. Lin, K.R. Tsai, J. Coord. Chem. 42 (1997) 131–141.
[127] Z.H. Zhou, H.L. Wan, S.Z. Hu, K.R. Tsai, Inorg. Chim. Acta 237 (1995) 193–197.
[128] D.W. Liao, Z.N. Huang, Y.Z. Lin, H.L. Wan, H.B. Zhang, K.R. Tsai, J. Chem. Inf. Comput. Sci. 36 (1996) 1178.